

# Some Examples of Family Floer Mirror

Man-Wai Cheung, Yu-Shen Lin

February 28, 2025

## Abstract

In this article, we give explicit calculations for the family Floer mirrors of some non-compact Calabi-Yau surfaces. We compare it with the mirror construction of Gross-Hacking-Keel-Siebert for suitably chosen log Calabi-Yau pairs and the rank two cluster varieties of finite type. In particular, the analytifications of the later two give partial compactifications of the family Floer mirrors that we computed.

## 1 Introduction

The Strominger-Yau-Zaslow (SYZ) conjecture predicts that Calabi-Yau manifolds have the structures of special Lagrangian fibration and the mirror can be constructed via dual special Lagrangian fibrations. Moreover, the Ricci-flat metrics of Calabi-Yau manifolds receive the instanton corrections from holomorphic discs with boundaries on the special Lagrangian torus fibres. The conjecture not only gives a geometric way to construct the mirror, it also gives the intuitive reasoning for mirror symmetry, for instance see [14, 35]. The SYZ philosophy becomes the helpful tool of studying mirror symmetry and many of its implications are proved. However, the difficulty of the analysis involving the singular special Lagrangian fibres makes the progress toward the original conjecture relatively slow (see [10, 11, 36] for the recent progress).

To understand the instanton correction rigorously in the mathematical context, Fukaya [17] proposed how to understand the relation between the instanton correction from holomorphic curves/discs and the mirror complex structure via the Floer theoretic approach. Kontsevich-Soibelman [32] and Gross-Siebert [28] later systematically formulated how to construct the mirror in various settings from algebraic approaches. These approaches opened up a window to understand mirror symmetry intrinsically.

In the algebro-geometric approach, Gross-Siebert first constructed an affine manifold with singularities from the toric degeneration of Calabi-Yau manifolds. Then there is a systematic way of constructing the so-called scattering diagrams, which capture the information of the instanton corrections, on the affine manifold. The data of the scattering diagrams encode how to glue the expected local models into the mirror Calabi-Yau manifolds. On the other hand, family Floer homology proposed by Fukaya [18] lays out the foundation to realize mirror symmetry via an intrinsic way from symplectic geometry point of view. Given a Lagrangian fibration, the Fukaya's trick introduced later in Section 4.1 provides pseudo-isotopies between the  $A_\infty$  structures of fibres after compensation of symplectic flux. In particular, the pseudo-isotopies induce canonical isomorphisms of the corresponding Maurer-Cartan spaces. The family Floer mirror is then the gluing of the Maurer-Cartan spaces via these isomorphisms. Not only the family Floer mirror are constructed [1, 44, 45, 46], Abouzaid proved the family Floer functor induces homological mirror symmetry [2, 3]. It is natural to ask if the mirrors constructed via Gross-Siebert program and the family Floer homology approach coincide or not.

The following is an expected dictionary connecting the two approaches:

<b>family Floer SYZ</b>	<b>GHKS mirror construction</b>
large complex structure limit	toric degeneration or Looijenga pair
base of SYZ fibration with complex affine structure	dual intersection complex of the toric degeneration or $B_{\text{GHK}}$
loci of SYZ fibres bounding holomorphic discs	rays in scattering diagram
homology of boundary of a holomorphic disc	direction of the ray
exp of generating function of open Gromov-Witten invariants of Maslov index zero	wall functions attached to the ray
coefficients of superpotential = open Gromov-Witten of Maslov index 2 discs	coefficients of theta functions = counting of broken lines
isomorphisms of Maurer-Cartan spaces induced by pseudo isotopies	wall crossing transformation
Lemma 4.1 in the article	consistency of scattering diagram
family Floer mirror	GHK/GHKS mirror

Table 1: Dictionary between the symplectic and algebraic approaches of mirror construction.

However, it is hard to have a good control of all possible discs in a Calabi-Yau manifold due to the wall-crossing phenomenon. Thus, it is generally hard to write down the family Floer mirror explicitly. In the examples family Floer mirror computed in the literature, there exist torus symmetries and one can write down all the possible holomorphic discs explicitly. In particular, the loci of Lagrangian fibres bounding Maslov index zero discs to not intersect and thus exclude the presence of more complicated bubbling phenomenon.

In this paper, we engineer some 2-dimensional examples that the family Floer mirrors can be computed explicitly and realize most part of the above dictionary step by step. We first prove that the complex affine structures of the bases of special Lagrangian fibrations coincide with the affine manifolds with singularities constructed in Gross-Hacking-Keel [24] from some log Calabi-Yau surfaces. See the similar results in [34] for the case of  $\mathbb{P}^2$ , general del Pezzo surfaces relative smooth anti-canonical divisors [33] and rational elliptic surfaces [11] and the case of Fermat hypersurfaces [36]. When a Calabi-Yau surface admits a special Lagrangian fibration, it is well-known that the special Lagrangian torus fibres bounding holomorphic discs are fibres above certain affine lines with respect to the complex affine coordinates on the base. Using the Fukaya's trick, the second author identified a version of open Gromov-Witten invariants with tropical discs counting [40, 37], which lays out a foundation to the connection between family Floer mirror and Gross-Siebert/Gross-Hacking-Keel mirror. The examples are engineer such that all the wall functions are polynomials. Therefore, there is no convergence issue in the gluing procedure and the complication is reduced to minimal. In particular, the family Floer mirror has a model over complex numbers. On the other hand, one can compare it with the process of Gross-Hacking-Keel: we can construct a log Calabi-Yau pair  $(Y, D)$  such that the induced affine manifold with singularity coincides with the complex affine structure of the base of special Lagrangian fibration. Then we identify the loci of special Lagrangian fibres bounding holomorphic discs with the rays of the canonical scattering diagram and the corresponding wall-crossing transformations in Gross-Hacking-Keel [24]. The technical part is to prove that the family Floer mirror has a partial compactification by the gluing of rigid analytic tori. Notice that if one directly compute the family Floer mirror of  $Y$  would lead to only a small subset of the mirror from Gross-Hacking-Keel mirror construction. One requires certain renormalization procedure (see [4][38]) and such machinery is not developed for family Floer mirror yet.

Comparing with the calculation of Gross-Hacking-Keel, we know that the family Floer mirror has a partial compactification to be the analytification of the mirror from  $(Y, D)$  constructed in Gross-Hacking-Keel. The mirror construction of Gross-Hacking-Keel is a family, which the base can be viewed as the complexified Kähler moduli of  $Y$ . We further determine the distinguished point that corresponds to the family Floer mirror. Denote  $Y'_*$  be the extremal rational elliptic surface with exactly two singular fibres and singular fibre over 0 in the base of type  $*$ , where  $*$  =  $II, III, IV$ . Let  $X'_*$  be the complement of the other

singular fibre. We will denote  $X_*$  be a suitable hyperKähler rotation of  $X'_*$ . The following is a summary of Theorem 5.23, Theorem 6.6 and Theorem 7.4

**Theorem 1.1.** *The analytification of  $\mathcal{X}$ -cluster variety of type  $A_2$  ( $B_2$  and  $G_2$ ) or the Gross-Hacking-Keel mirror of suitable log Calabi-Yau pair  $(Y, D)$  is a partial compactification of the family Floer mirror of  $X_{II}$  ( $X_{III}$  and  $X_{IV}$  respectively).*

Except for being the first example of explicitly computation of family Floer mirror without  $S^1$ -symmetries and the comparison of two mirror constructions, the above theorem has other significance. For instance, it is not clear the Gross-Hacking-Keel mirror in general would satisfy the homological mirror symmetry. On the other hand, the family Floer mirror is designed to prove the homological mirror symmetry conjecture. Abouzaid proved that (when there is no singular fibre) the family Floer mirrors make the homological mirror symmetry conjecture hold [3]. The comparison of the two mirror constructions provides an intermediate step towards the homological mirror symmetry for Gross-Hacking-Keel mirrors.

## 1.1 Structure

The structure of the paper is arranged as follows: In Section 2, we review the definition of cluster varieties and the mirror construction in Gross-Hacking-Keel [24] and Gross-Hacking-Keel-Siebert [27]. In Section 3, we will formulate the surfaces that we are going to compute the family Floer mirror of those. They are coming from the HyperKähler rotation of the rational elliptic surfaces with prescribed singularities.

In Section 4, we review the family Floer mirror construction and the relation between the open Gromov-Witten invariants. In Section 5, we will compute the family Floer mirror of a non-compact Calabi-Yau surface  $X_{II}$  explicitly in full details. Then we compare it with the analytification of the  $A_2$ -cluster variety. We will also compare it with the Gross-Hacking-Keel mirror for a del Pezzo surface of degree five. In particular, the family Floer mirror of  $X_{II}$  can compactified to a del Pezzo surface of degree five via algebra structure of the theta functions. In Section 6 and Section 7, we will sketch the calculation for the family Floer mirror of  $X_{III}$  and  $X_{IV}$ , pointing out the differences from the case of  $X_{II}$ .

## Acknowledgement

The author would like to thank Mark Gross and Shing-Tung Yau for the constant support and encouragement. The authors would also like to thank Hülya Argüz, Dori Bejleri, Paul Hacking, Hansol Hong, Chi-Yun Hsu, Laura Friedrickson, Tom Sutherland for helpful discussion. The first author is supported by NSF grant DMS-1854512. The second author is supported by Simons Collaboration Grant # 635846.

## 2 Cluster Varieties and GHK Mirrors

### 2.1 Gross-Hacking-Keel Mirror Construction

An important novelty of Gross-Hacking-Keel [24] is that the enumerative invariants from  $\mathbb{A}^1$ -curves in a log Calabi-Yau surface already recover its mirror family. Heuristically, as the SYZ fibres moved to infinity in a direction, the Maslov index zero holomorphic discs with suitable boundary homology class close up to holomorphic curves with exactly one intersection with some boundary divisor and become the  $\mathbb{A}^1$ -curves. The  $\mathbb{A}^1$ -curves tropicalize to rays and the counting of  $\mathbb{A}^1$ -curves will determine the wall functions of the canonical scattering diagram. In this section, we will review the mirror construction of Gross-Hacking-Keel [24] and Gross-Hacking-Keel-Siebert [27].

Consider the pair  $(Y, D)$ , where  $Y$  is a smooth projective rational surface, and  $D = D_1 + \cdots + D_n$  is an anti-canonical cycle of rational curves. Then  $X := Y \setminus D$  is a log Calabi-Yau surface<sup>1</sup>. The tropicalization of  $(Y, D)$  would be a pair  $(B_{\text{GHK}}, \Sigma)$ , where  $B_{\text{GHK}}$  is homeomorphic to  $\mathbb{R}^2$  and has the structure of integral affine manifold with singularity at the origin, and  $\Sigma$  is a decomposition of  $B_{\text{GHK}}$  into cones. The construction of  $(B_{\text{GHK}}, \Sigma)$  starts by associating each node  $p_{i,i+1} := D_i \cap D_{i+1}$  with a rank two lattice  $M_{i,i+1}$  with basis

<sup>1</sup>Note that  $X$  is denoted as  $U$  in [24, 27].

$v_i, v_{i+1}$  and the cone  $\sigma_{i,i+1} \subset M_{i,i+1} \otimes_{\mathbb{Z}} \mathbb{R}$  generated by  $v_i$  and  $v_{i+1}$ . Then  $\sigma_{i,i+1}$  are glued to  $\sigma_{i-1,i}$  along the rays  $\rho_i := \mathbb{R}_{\geq} v_i$  to obtain a piecewise-linear manifold  $B_{\text{GHK}}$  and a decomposition

$$\Sigma = \{\sigma_{i,i+1} | i = 1, \dots, n\} \cup \{\rho_i | i = 1, \dots, n\} \cup \{0\} \subseteq \mathbb{R}^2.$$

Define

$$U_i = \text{Int}(\sigma_{i-1,i} \cup \sigma_{i,i+1}).$$

The integral affine structure on  $B_{\text{GHK},0} = B_{\text{GHK}} \setminus \{0\}$  is defined by the charts

$$\psi : U_i \rightarrow M_{\mathbb{R}},$$

$$\psi(v_{i-1}) = (1, 0), \quad \psi(v_i) = (0, 1), \quad \psi(v_{i+1}) = (-1, -D_i^2),$$

with  $\psi_i$  linear on  $\sigma_{i-1,i}$  and  $\sigma_{i,i+1}$ . It may worth noting here that at the end of the gluing process,  $\rho_{n+1}$  may not agree with  $\rho_1$ . It would induce a nontrivial affine structure on  $B_{\text{GHK},0}$  when we identify  $\rho_{n+1}$  with  $\rho_1$ . We are going to demonstrate the affine structures explicitly in examples later in this article. Heuristically, one scales the neighborhood of the infinity or equivalently collides all the singular fibres of the SYZ fibration into one to achieve  $B_{\text{GHK}}$ . Note that if we consider three successive rays  $\rho_{i-1}, \rho_i, \rho_{i+1}$ , there is the relation

$$\psi(v_{i-1}) + D_i^2 \psi(v_i) + \psi(v_{i+1}) = 0. \quad (1)$$

Consider a toric monoid  $P$ . A toric monoid  $P$  is a commutative monoid whose Grothendieck group  $P^{\text{gp}}$  is a finitely generated free abelian group and  $P = P^{\text{gp}} \cap \sigma_P$ , where  $\sigma_P \subseteq P^{\text{gp}} \otimes_{\mathbb{Z}} \mathbb{R} = P_{\mathbb{R}}^{\text{gp}}$  is a convex rational polyhedral cone. We will assume that  $P$  comes with a homomorphism  $\eta : \text{NE}(Y) \rightarrow P$  of monoids, where  $\text{NE}(Y)$  is the intersection of the cone generated by effective curves with  $A_1(Y, \mathbb{Z})$ . In later discussion, we will in particular choose  $P = \text{NE}(Y)$  and  $\eta$  to be the identity.

Next we define a multi-valued  $\Sigma$ -piecewise linear function as a continuous function  $\varphi : |\Sigma| \rightarrow P_{\mathbb{R}}^{\text{gp}}$  such that for each  $\sigma_{i,i+1} \in \Sigma_{\text{max}}$ ,  $\varphi_i = \varphi|_{\sigma_{i,i+1}}$  is given by an element  $\varphi_{\sigma_{i,i+1}} \in \text{Hom}_{\mathbb{Z}}(M, P^{\text{gp}}) = N \otimes_{\mathbb{Z}} P^{\text{gp}}$ . For each codimension cone  $\rho = \mathbb{R}_{+} v_i \in \Sigma$  contained in two maximal cones  $\sigma_{i-1,i}$  and  $\sigma_{i,i+1}$ , we have

$$\varphi_{i+1} - \varphi_i = n_{\rho} \otimes [D_i], \quad (2)$$

where  $n_{\rho} \in N$  is the unique primitive element annihilating  $\rho$  and positive on  $\sigma_{i,i+1}$ . Such data  $\{\varphi_i\}$  gives a local system  $\mathcal{P}$  on  $B_{\text{GHK},0}$  with the structure of  $P_{\mathbb{R}}^{\text{gp}}$ -principal bundle  $\pi : \mathbb{P}_0 \rightarrow B_{\text{GHK},0}$ . To determine such a local system, we first construct an affine manifold  $\mathbb{P}_0$  by gluing  $U_i \times P_{\mathbb{R}}^{\text{gp}}$  to  $U_{i+1} \times P_{\mathbb{R}}^{\text{gp}}$  along  $(U_i \cap U_{i+1}) \times P_{\mathbb{R}}^{\text{gp}}$  by

$$(x, p) \mapsto (x, p + \varphi_{i+1}(x) - \varphi_i(x)).$$

The local sections  $x \mapsto (x, \varphi_i(x))$  patch to give a piecewise linear section  $\varphi : B_{\text{GHK},0} \rightarrow \mathbb{P}_0$ . Let  $\Lambda_B$  denote the sheaf of integral constant vector fields, and  $\Lambda_{B,\mathbb{R}} := \Lambda_B \otimes_{\mathbb{Z}} \mathbb{R}$ . We can then define

$$\mathcal{P} := \pi_* \Lambda_{B,\mathbb{P}_0} \cong \varphi^{-1} \Lambda_{B,\mathbb{P}_0}$$

on  $B_{\text{GHK},0}$ . There is an exact sequence

$$0 \rightarrow \underline{P}^{\text{gp}} \rightarrow \mathcal{P} \xrightarrow{r} \Lambda_B \rightarrow 0 \quad (3)$$

of local systems on  $B_{\text{GHK},0}$ , where  $r$  is the derivative of  $\pi$ . Then (2) is equivalent to

$$\varphi_i(v_{i-1}) + \varphi_i(v_{i+1}) = [D_i] - D_i^2 \varphi_i(v_i), \quad (4)$$

which is the lifting of (1) to  $\mathcal{P}$ . We will describe the symplectic meaning of  $P$ ,  $P^{\text{gp}}$ , and  $\mathcal{P}$  in Section 5.2, particularly see (47).

Next one would define the canonical scattering diagram  $\mathfrak{D}_{\text{can}}$  on  $(B_{\text{GHK}}, \Sigma)$ . We will first state the definition of scattering diagram as in [27] and then restrict to the finite case in this article. A ray in  $\mathfrak{D}_{\text{can}}$  is a pair  $(\mathfrak{d}, f_{\mathfrak{d}})$  where

- $\mathfrak{d} \subset \sigma_{i,i+1}$  for some  $i$ , called the support of a ray, is a ray generated by  $av_i + bv_{i+1} \neq 0$ ,  $a, b \in \mathbb{Z}_{\geq 0}$ ;

- $\log f_{\mathfrak{d}} = \sum_{k \geq 1} k c_k X_i^{-ak} X_{i+1}^{-bk} \in \mathbb{k}[P][[X_i^{-a} X_{i+1}^{-b}]]$  with <sup>2</sup>  $c_k$  in the maximal ideal  $\mathfrak{m} \subseteq \mathbb{k}[P]$ .

The coefficient  $c_k$  is the generating function of relative Gromov-Witten invariants,

$$c_k = \sum_{\beta} N_{\beta} z^{\beta},$$

where the summation is over all possible classes  $\beta \in H_2(Y, \mathbb{Z})$  with incidence relation  $\beta.D_i = ak, \beta.D_{i+1} = bk$  and  $\beta.D_j = 0$ , for  $j \neq i, i+1$ . The coefficient  $N_{\beta}$  is the counting of  $\mathbb{A}^1$ -curves in such class  $\beta$ . We will refer the readers to [24, Section 3] for technical details of the definition of the relative Gromov-Witten invariants.

Roughly speaking, a scattering diagram for the data  $(B_{\text{GHK}}, \Sigma)$  is a set  $\mathfrak{D}_{\text{can}} = \{(\mathfrak{d}, f_{\mathfrak{d}})\}$  such that there are only finitely many  $f_{\mathfrak{d}} \neq 1$ . Note that scattering diagrams may give a refinement to the original fan structure given by  $\Sigma$ . We will call the maximal cones of this refinement as chambers.

The scattering diagram will lead to a flat family over  $\text{Spec } A_I$ , where  $A_I = \mathbb{k}[P]/I$  and  $I \subseteq \mathbb{k}[P]$  is any monomial ideal with  $\mathbb{k}[P]/I$  is Artinian. Now consider each  $\rho_i$  as the support of a ray  $(\rho_i, f_i)$  in  $\mathfrak{D}_{\text{can}}$ . Define

$$\begin{aligned} R_{i,I} &:= A_I[X_{i-1}, X_i^{\pm 1}, X_{i+1}]/(X_{i-1}X_{i+1} - z^{[D_i]}X_i^{-D_i^2}f_i), \\ R_{i,i+1,I} &:= A_I[X_i^{\pm 1}, X_{i+1}^{\pm 1}] \cong (R_{i,I})_{X_{i+1}}, \end{aligned}$$

where  $z^{[D_i]}$  is the monomial in  $\mathbb{k}[P]$  corresponding to the class of  $[D_i]$ . Let

$$U_{i,I} := \text{Spec } R_{i,I} \text{ and } U_{i,i+1,I} = \text{Spec } R_{i,i+1,I}.$$

Notice that the fibre of  $U_{i,i+1,I} \rightarrow \text{Spec } A_I$  over a closed point is a torus  $\mathbb{G}_m^2$ . Directly computation shows that the fibre of  $U_{i,I} \rightarrow \text{Spec } A_I$  over a closed point is the partial compactification of graph of the birational map

$$\begin{aligned} U_{i-i,i,I} &\dashrightarrow U_{i,i+1,I} \\ (X_{i-1}, X_i) &\mapsto (X_{i+1}^{-1}z^{[D_i]}X_i^{-D_i^2}f_i, X_i). \end{aligned} \quad (5)$$

In particular, the the fibre of  $U_{i,I} \rightarrow \text{Spec } A_I$  is the graph of (5) up to codimension two if  $V(f_i) \neq \emptyset$ . One would then like to glue  $U_{i,I}$  and  $U_{i+1,I}$  over the identified piece  $U_{i,i+1,I}$  to obtain a scheme  $X_I^{\circ}$  flat over  $\text{Spec } A_I$ .

To obtain a better behaved  $X_I^{\circ}$ , one needs to consider an automorphism  $R_{i,i+1,I}$ , called the path ordered product, associated to a path  $\gamma : [0, 1] \rightarrow \text{Int}(\sigma_{i,i+1})$ . Suppose  $\gamma$  crosses a given ray  $(\mathfrak{d} = \mathbb{R}_{\geq 0}(av_i + bv_{i+1}), f_{\mathfrak{d}})$ . The  $A_I$ -algebra homomorphism  $\theta_{\gamma, \mathfrak{d}} : R_{i,i+1,I} \rightarrow R_{i,i+1,I}$  is defined by  $X_i^{k_i} X_{i+1}^{k_{i+1}} \mapsto X_i^{k_i} X_{i+1}^{k_{i+1}} f_{\mathfrak{d}}^{\pm(-bk_i + ak_{i+1})}$ , where the sign  $\pm$  is positive if  $\gamma$  goes from  $\sigma_{i-1,i}$  to  $\sigma_{i,i+1}$  when passing through  $\mathfrak{d}$ ; it is negative if  $\gamma$  goes in the opposite direction and one can see this is the same as the wall crossing transformation stated in (12). If  $\gamma$  passes through more than one ray, one defines the path ordered product as composing each individual path ordered product of each ray in the order according to the order of rays the  $\gamma$  passes. Choosing a path  $\gamma$  by starting very close to  $\rho_i$  and ending near  $\rho_{i+1}$  in  $\sigma_{i,i+1}$ , then  $\gamma$  would pass all the rays in  $\sigma_{i,i+1}$ . Then define  $X_{I,\mathfrak{D}}^{\circ} = \coprod_i U_{i,I} / \sim$  with the gluing given by

$$U_{i,I} \hookleftarrow U_{i,i+1,I} \xrightarrow{\theta_{\gamma, \mathfrak{D}}} U_{i,i+1,I} \hookrightarrow U_{i+1,I}.$$

The following observation is important later for the comparison between the Gross-Hacking-Keel mirror with the family Floer mirror in the examples consider in this paper.

**Remark 2.1.** *When there are only finitely many rays  $\mathfrak{d}$  with nontrivial  $f_{\mathfrak{d}}$  and  $I = \mathfrak{m}$ , one can replace  $(Y, D)$  by a minimal resolution such that all the  $\mathbb{A}^1$ -curves are transversal to the toric boundary divisors. The procedure replaces  $\Sigma$  by the refinement given by the original canonical scattering diagram and the integral affine manifold  $B_{\text{GHK}}$  is remained the same. Then  $X_{I,\mathfrak{D}}^{\circ}$  is gluing of tori, one corresponds to a chamber.*

<sup>2</sup>At first glance, it looks like there is a sign change comparing with the wall functions of the scattering diagram from Floer theory in Definition 4.3. However, such discrepancy is explained in the discussion after Lemma 5.22

The next step in [24, 27] is considering the broken lines to define consistency and to construct the theta functions. Since we will focus on the finite type in this paper, we can make use of path-ordered product directly without the use of broken lines. For the definition of broken lines and theta functions, one can refer to [24, Section 2.2]. Instead, to define consistency, we can extend the definition of path ordered product to the path  $\gamma : [0, 1] \rightarrow B_0(\mathbb{Z})$  with starting point  $q$ , and end point  $Q$ , where  $q$  and  $Q$  do not lie on any ray. Then the path ordered product  $\theta_{\gamma, \mathfrak{D}}$  can be defined similarly by composing  $\theta_{\gamma, \mathfrak{d}}$ 's of the walls  $\mathfrak{d}$  passed by  $\gamma$ . Then the canonical scattering diagram  $\mathfrak{D}$  is consistent in the sense that the path ordered product  $\theta_{\gamma, \mathfrak{D}}$  only depends on the two end points  $q$  and  $Q$ .

For a point  $q \in B_0(\mathbb{Z})$ , let us assume  $q = av_{i-1} + bv_i \in \sigma_{i-1, i}$  and associate the monomial  $X_{i-1}^a X_i^b$  to  $q$ . Consider now another point  $Q \in \sigma_{i, i+1} \setminus \bigcup_{\mathfrak{d} \in \mathfrak{D}_{lim}} \text{Supp} \mathfrak{d}$  and a path  $\gamma$  from  $\sigma_{i-1, i}$  to  $\sigma_{i, i+1}$ . We will define  $\vartheta_{q, Q} = \left( z^{[D_i]} X_i^{-D_i^2} f_i X_{i+1}^{-1} \right)^a X_i^b$ . Note that the variables in  $R_{i-1, i, I}$  are  $X_{i-1}, X_i$  while the variables in  $R_{i, i+1, I}$  are  $X_i, X_{i+1}$ . The change of variables are described the gluing from  $R_{i, I}$ . We will do similarly if the  $\gamma$  goes in the opposite direction. Further if  $q, Q \in B_0(\mathbb{Z})$  not in adjacent chambers, we can consider a path  $\gamma$  from  $q$  to  $Q$  and define  $\vartheta_{q, Q}$  by composing the changes of variables from the order of the chambers of how  $\gamma$  runs around  $\mathfrak{D}$ . This is well-defined since we have assumed our scattering diagram  $\mathfrak{D}$  is consistent. We will define  $\vartheta_{0, Q} = \vartheta_0 = 1$ . Thus the  $\vartheta_{q, Q}$  for various  $Q$  can be glued to give the global function  $\vartheta_q \in \Gamma(X_{I, \mathfrak{D}}^\circ, \mathcal{O}_{X_{I, \mathfrak{D}}^\circ})$ . Then, by [24, Theorem 2.28],  $X_{I, \mathfrak{D}} := \text{Spec } \Gamma(X_{I, \mathfrak{D}}^\circ, \mathcal{O}_{X_{I, \mathfrak{D}}^\circ})$  is a partial compactification of  $X_{I, \mathfrak{D}}^\circ$ .

## 2.2 Cluster varieties

Gross-Hacking-Keel-Kontsevich [26] constructed the cluster scattering diagrams and showed that the cluster monomials can be expressed as theta functions defined on the cluster scattering diagrams. The collections of the theta functions form the bases to the (middle) cluster algebras defined by Fomin-Zelevinsky [15].

One can perform the similar construction as in the Gross-Hacking-Keel mirror construction by associating each chamber in the cluster scattering diagram with an algebraic torus. The path-ordered products (wall crossings) give the birational maps between the tori. The  $\mathcal{A}_{\text{prin}}$ -cluster varieties are then defined as the schemes (up to codimension 2) obtained from gluing the tori associated to the chambers by the birational maps. The  $\mathcal{X}$ -cluster varieties can be described as quotient of the  $\mathcal{A}_{\text{prin}}$ -varieties by torus action. The reader can refer to [25] for detail definition of cluster varieties.

We can define the  $\mathcal{A}_{\text{prin}}$ -scattering diagrams, and  $\mathcal{A}$ -scattering diagram if the injectivity assumption. One can define the  $\mathcal{X}$  scattering diagram as quotient of the  $\mathcal{A}_{\text{prin}}$ -scattering diagrams as described in [8]. Note that the underlying affine manifolds of the cluster scattering diagrams do not carry any monodromy which are not exactly the same as canonical scattering diagrams. The cluster scattering diagrams can be seen as pushing the singularities of the affine structures of  $B$  of canonical scattering diagrams to infinity as explained in [9]. We will illustrate how to choose branch cuts and decompose the monodromy of  $B$  in Section 5.3. Then we can translate from the canonical scattering diagrams to the cluster scattering diagrams. The resulting schemes, no matter described by the canonical or the cluster scattering diagrams, are determined (up to codimension 2) by the algebras generated by the set of theta functions. We are going to see the cases in this article are all associated to cluster algebras.

For the dimension two case, the fix data <sup>3</sup> are given by the bilinear form  $\begin{pmatrix} 0 & 1 \\ -1 & 0 \end{pmatrix}$  and the scalars  $d_1, d_2 \in \mathbb{N}$ . Given fixed data, we can define the  $\mathcal{A}$  (and  $\mathcal{X}$ ) cluster varieties such that the rings of regular functions carry the  $\mathcal{A}$  (and  $\mathcal{X}$ ) cluster structures respectively. Gross-Hacking-Keel-Kontsevich [26] showed that the middle  $\mathcal{A}$  and  $\mathcal{X}$  cluster algebras can be constructed from the theta functions of the corresponding schemes. Relations between the generators  $\vartheta_i$  in the cluster complex of the (middle)  $\mathcal{X}$  cluster algebras can be expressed as

$$\vartheta_{i-1} \cdot \vartheta_{i+1} = \begin{cases} (1 + \vartheta_i)^{d_1}, & \text{if } i \text{ is odd} \\ (1 + \vartheta_i)^{d_2}, & \text{if } i \text{ is even,} \end{cases} \quad (6)$$

where  $i \in \mathbb{Z}$ . Conversely, given such relations between the variables, we can determine the algebras.

<sup>3</sup>We follow the definition of fixed data as in [25]

### 3 Set-Up of the Geometry

Consider  $Y'$  an extremal rational elliptic surface with its singular configuration one of the following:  $II^*II$ ,  $III^*III$ ,  $IV^*IV$ ,  $I_0^*I_0^*$ . Here we use the notation in the Kodaira classification of the singular fibres. We will denote  $Y' = Y'_*$ , where  $*$  =  $II, III$  or  $IV$  be the fibre over zero. These rational elliptic surfaces can be constructed explicitly.

We will first consider the case  $Y'$  is the unique rational elliptic surface with singular configuration  $II^*II$ . The surface  $Y'$  can be constructed as the minimal resolution of the surface

$$\{ty^2z = tx^3 + atxz^2 + uz^3\} \subseteq \mathbb{P}_{(x,y,z)}^2 \times \mathbb{P}_{(u,t)}^1. \quad (7)$$

By the Tate algorithm [43],  $Y'$  is an elliptic surface with a type  $II^*$  singular fibre over  $u = \infty$ . Straight-forward calculation shows that  $Y'$  has singular configuration  $II^*I_1^2$  if  $a \neq 0$  and  $II^*II$  if  $a = 0$  and produce the extremal rational elliptic surface  $Y'_{II}$ . By the Calstelnuvo's criterion of rationality,  $Y'$  is rational and thus an rational elliptic surface. The other extremal rational elliptic surfaces can be constructed similarly with the corresponding affine equations below [41, p.545]:

$$\begin{aligned} y^2 &= x^4 + u \\ y^2 &= x^3 + t^2s^4 \\ y^2 &= x^3 + at^2s^2x + bt^3s^4. \end{aligned}$$

It seems to the authors that the above examples are closely related to the geometry from  $SU(2)$  gauge theory studied in [21].

Recall that any rational elliptic surface  $Y'$  has canonical bundle  $K_{Y'} = \mathcal{O}_{Y'}(-D')$ , where  $D'$  denotes an elliptic fibre. Thus, there exists a meromorphic 2-form  $\Omega'$  with simple pole along an assigned fibre which is unique up to a  $\mathbb{C}^*$ -scaling. In particular, the non-compact surface  $X' = Y' \setminus D'$  can be viewed as an non-compact Calabi-Yau surface. Indeed,

**Theorem 3.1.** [30] *There exists a Ricci-flat Kähler form  $\omega'$  on  $X'$  for any choice of the fibre  $D'$ . In particular,  $2\omega'^2 = \Omega' \wedge \bar{\Omega}'$  and  $X'$  is hyperKähler.*

The Ricci-flat Kähler form may not be unique (even in a given cohomology class), but we will just fix one for the later purpose and family Floer mirror computations will not affect by such choices. Consider  $D'_*$  to be the infinity fibre in  $Y'_*$  and denote the hyperKähler rotation of  $X'_* = Y'_* \setminus D'_*$  by  $X = X_*$ . Explicitly,  $X_*$  has the same underlying space as  $X'_*$  and equipped with the Kähler form and the holomorphic volume form

$$\begin{aligned} \omega &= \text{Re}\Omega' \\ \Omega &= \omega' - i\text{Im}\Omega'. \end{aligned} \quad (8)$$

Then the elliptic fibration  $X'_* \rightarrow \mathbb{C}$  becomes the special Lagrangian fibration  $X_* \rightarrow B$ , where  $B \cong \mathbb{R}^2$  [29] (see the diagram below) topologically. Let  $B_0 \cong \mathbb{R}^2 \setminus \{0\}$  be the complement of the discriminant locus. We will refer the readers to [10, P.35] for more explicit calculation of hyperKähler (HK) rotation. We will omit the subindex when there is no confusion.

$$\begin{array}{ccccc} Y' & \longleftrightarrow & X' = Y' \setminus D' & \xleftarrow{\text{HK}} & X \\ \downarrow & & \downarrow & & \downarrow \\ \mathbb{P}^1 & \longleftrightarrow & B \cong \mathbb{C} & \longrightarrow & B \cong \mathbb{R}^2 \end{array}$$

The fibrewise relative homology  $H_2(X, L_u)$  glues to a local system of lattices over  $B_0$ . For any relative class  $\gamma \in H_2(X, L_u)$ , we denote the central charge

$$Z_\gamma(u) := \int_\gamma \Omega'$$

be a function from the local system  $\Gamma$  to  $\mathbb{C}$ . Notice that  $B_0 \cong \mathbb{C}^*$  admits a complex structure structure and  $Z_\gamma$  is locally<sup>4</sup> a holomorphic function in  $u$  by Corollary 2.8 [38]. The central charge will help to locate the special Lagrangian torus fibre bounding holomorphic discs in Section 4.2.

<sup>4</sup>Since there is monodromy, it is a multi-value function on  $B_0$

### 3.1 Affine Structures of the Base

Let  $(X, \omega)$  be a Kähler surface with holomorphic volume form  $\Omega$  satisfying  $2\omega^2 = \Omega \wedge \bar{\Omega}$ . Assume that  $X$  admits a special Lagrangian fibration  $X \rightarrow B$  possibly with singular fibres with respect to  $(\omega, \Omega)$ , i.e.,  $\omega|_L = \text{Im}\Omega|_L = 0$  for any fibre  $L$ . We will use  $L_u$  to denote the fibre over  $u \in B$ . There are two natural integral affine structures defined on  $B_0$  by Hitchin [31], one is called the symplectic affine structure and the other one is the complex affine structure. Given a reference point  $u_0 \in B_0$  and a choice of the basis  $\check{e}_1, \check{e}_2 \in H_1(L_{u_0}, \mathbb{Z})$ , we will define the local affine coordinates around  $u_0$ . For any  $u \in B_0$  in a small neighborhood of  $u_0$ , one choose a path  $\phi$  contained in  $B_0$  connecting  $u, u_0$ . Let  $C_k$  to be the  $S^1$ -fibration over the image of  $\phi$  such that the fibres are in the homology class of parallel transport of  $\check{e}_k$  along  $\phi$ . Then the local symplectic affine coordinates are defined by

$$x_k(u) = \int_{C_k} \omega. \quad (9)$$

It is straight-forward to check that the transition functions fall in  $GL(2, \mathbb{Z}) \rtimes \mathbb{R}^2$ , and thus the above coordinates give an integral affine structure on  $B_0$ .

**Remark 3.2.** *From the construction, primitive classes  $\check{e} \in H_1(L_u, \mathbb{Z})$  are in one-to-one correspondence with the primitive integral vectors in  $(T_{\mathbb{Z}}B_0)_u$ . Indeed, each  $v \in T_u B_0$  has a corresponding functional  $\int_{-} \iota_v \text{Im}\Omega$  on  $H_1(L_u, \mathbb{Z})$  and thus corresponds to a primitive element in  $H_1(L_u, \mathbb{Z})$  via its natural symplectic pairing and Poincare duality.*

If there is a global Lagrangian section, then the transition functions fall in  $GL(2, \mathbb{Z})$ . One can replace  $\omega$  in (9) by  $\text{Im}\Omega$ , then one gets the complex integral affine coordinates  $\check{x}_k(u)$ .

**Remark 3.3.** *Since special Lagrangians have vanishing Maslov classes, all the special Lagrangian torus fibres only bound Maslov index zero discs and the assumption of the Lemma 4.1 holds. In general, it is hard to control all the bubbling of pseudo-holomorphic discs (of Maslov index zero). However, when the Lagrangian fibration is further special, the loci of special Lagrangian fibres bounding holomorphic discs of a fixed relative class falls in an affine line with respect to the complex affine structure. Indeed, if  $u_t$  be a path in  $B_0$  such that each  $L_{u_t}$  bounds a holomorphic disc in class  $\gamma$  (we identify the relative classes via parallel transport along the path  $u_t$ ) for every  $t$ , then  $\int_{\gamma} \text{Im}\Omega = 0$  along  $u_t$ . In particular,  $u_t$  is contained in an affine line with respect to the complex affine structure, which locally we will denote it by  $l_{\gamma}$ <sup>5</sup>. Notice that  $l_{\gamma}$  is naturally oriented such that the symplectic area of  $\gamma$  is increasing along  $l_{\gamma}$ . From the expected dictionary in the introduction, these affine lines correspond to the rays in the scattering diagrams and the Lemma 4.1 translates to the consistency of scattering diagrams.*

We will use both integral affine structures later: the complex affine structures will be used to locate the fibres bounding holomorphic discs (see Section 4.2) while the symplectic affine structures will be used to define the family Floer mirrors (see Section 4.3).

## 4 Floer Theory and Family Floer Mirror

In this section, we will talk about the background for the explicit calculation of the family Floer mirror in Section 5. We will review the construction of family Floer mirror of Tu [44] in Section 4.3. Given a Lagrangian torus fibration  $X \rightarrow B$  with fibre  $L_u$  over  $u \in B$ , Fukaya-Oh-Ohta-Ono [20] constructed  $A_{\infty}$  algebras on de Rham cohomologies of the fibres. Assume that the fibres are unobstructed, then the exponential of the corresponding Maurer-Cartan spaces are the analogue of the dual tori for the original Lagrangian fibration. Then the family Floer mirror are gluing of these exponential of Maurer-Cartan spaces. The gluing morphisms, known as the "quantum correction" to the mirror complex structure, are induced by the wall-crossing of the Maurer-Cartan spaces. Such wall-crossing phenomenons receive contribution from the holomorphic discs of Maslov index zero with boundaries on SYZ fibres. We review the relation of the

<sup>5</sup>The notation  $\gamma$  and thus  $l_{\gamma}$  are only locally define due to the monodromy of the fibration act non-trivially on the local system  $\bigcup_{u \in B_0} H_2(X, L_u)$



open Gromov-Witten invariants with the gluing morphisms in Section 4.1. To have better understanding of the gluing morphisms, in Section 4.2 we study the location of all fibres with non-trivial open Gromov-Witten invariants within the geometry discussed in Section 3 by taking advantage of the special Lagrangina boundary conditions.

#### 4.1 Fukaya's Trick and Open Gromov-Witten Invariants

We will first review the so-called Fukaya's trick, which is a procedure to compare the variation of the  $A_\infty$  structures of a Lagrangian and those of its nearby deformations. We will use the Fukaya's trick to detect the open Gromov-Witten invariants.

Let  $X$  be a symplectic manifold with Lagrangian fibration  $X \rightarrow B$ . Recall the definition of Novikov field,

$$\Lambda := \left\{ \sum_{i \in \mathbb{N}} c_i T^{\lambda_i} \mid \lambda_i \in \mathbb{R}, \lim_{i \rightarrow \infty} \lambda_i = \infty, c_i \in \mathbb{C} \right\}.$$

Denote  $\Lambda_+ = \{\sum_{i \in \mathbb{N}} c_i T^{\lambda_i} \mid \lambda_i > 0\}$  and  $\Lambda^* = \Lambda \setminus \{0\}$ . There is a natural discrete valuation

$$\begin{aligned} \text{val} : \Lambda^* &\longrightarrow \mathbb{R} \\ \sum_{i \in \mathbb{N}} c_i T^{\lambda_i} &\mapsto \lambda_{i_0}, \end{aligned}$$

where  $i_0$  is the smallest  $i$  with  $\lambda_i \neq 0$ . One can extend the domain of  $\text{val}$  to  $\Lambda$  by setting  $\text{val}(0) = \infty$ .

Let  $B_0$  be the complement of the discriminant locus of the special Lagrangian fibration and  $L_u$  be the fibre over  $u \in B_0$ . Fix an almost complex structure  $J$  which is compatible with  $\omega$ . For the later purpose,  $X$  will be Kähler and we will take  $J$  to be its complex structure. Given a relative class  $\gamma \in H_2(X, L_u)$ , we use  $\mathcal{M}_\gamma((X, J), L_u)$  to denote the moduli space of stable  $J$ -holomorphic discs in relative class  $\gamma$  with respect to the almost complex structure  $J$ . We may omit the  $J$  if there is no confusion. Fukaya-Oh-Ohta-Ono [20] constructed a filtered unital  $A_\infty$  structure  $\{m_k\}_{k \geq 0}$  on  $H^*(L_u, \Lambda)$  by considering the boundary relations of  $\mathcal{M}_\gamma((X, L), L_u)$ , for all  $\gamma \in H_2(X, L_u)$ . We will assume that there exists only Maslov index zero discs in  $X$ . If we restrict to  $\dim_{\mathbb{R}} X = 4$ , then due to the dimension reason, the moduli space  $M_\gamma((X, J), L_u)$  has virtual dimension negative one. In particular, the Maurer-Cartan space associate to the  $A_\infty$  structure is simply  $H^1(L_u, \Lambda_+)$ .

Now we explain the so-called Fukaya's trick. Given  $p \in B_0$  and a path  $\phi$  contained in a small neighborhood of  $p$  such that  $\phi(0) = u_-$ ,  $\phi(1) = u_+$ . One can choose a 1-parameter family of paths  $\phi_s(t)$  such that  $\phi_s(t)$  is a path from  $\phi(t)$  to  $p$  and  $\phi_s(t)$  is contained in a small enough neighborhood of  $p$ . It is illustrated as follow:

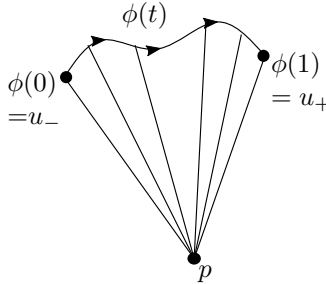


Figure 1: Fukaya's trick

Then there exists a 2-parameter family of fibrewise preserving diffeomorphisms  $f_{s,t}$  such that

1.  $f_{s,1} = id$ .
2.  $f_{s,t}$  sends  $L_{\phi_s(t)}$  to  $L_p$ .
3.  $f_{s,t}$  is an identity outside the preimage of a compact subset of  $B_0$ .

Then  $J_t = (f_{1,t})_* J$  is a 1-parameter family of almost complex structures tamed with respect to  $\omega$  since  $\phi$  is contained in a small enough neighborhood of  $p$ . There is a canonical isomorphism of moduli spaces of holomorphic discs

$$\mathcal{M}_{k,\beta}((X, J), L_{\phi(t)}) \cong \mathcal{M}_{k,(f_{1,t})_*\beta}((X, (f_{1,t})_* J), L_p) \quad (10)$$

which carries over to the identification of the Kuranishi structures. However, the  $A_\infty$  from two sides of (10) structures are not the same under the parallel transport  $H^*(L_{\phi(t)}, \Lambda) \cong H^*(L_p, \Lambda)$  because of the difference of the corresponding symplectic area (or known as the flux)

$$\int_{f_{1,t,*}\beta} \omega - \int_\beta \omega = \left\langle \sum_{k=1}^n (x_k(\phi(t)) - x_k(p)) e_k, \partial\beta \right\rangle,$$

where  $e_i \in H^1(L_p, \mathbb{Z})$  is an integral basis.

From the 1-parameter family of almost complex structures  $J_t$ , one can construct a pseudo-isotopy of unital  $A_\infty$  structures on  $H^*(L_p, \Lambda)$ , connecting the  $A_\infty$  structures on  $H^*(L_p, \Lambda)$  from  $u_\pm$  (for instance see [19]). This induces a pseudo-isotopy of the  $A_\infty$  structures from  $H^*(L_p, \Lambda)$  to itself. In particular, this induces an isomorphism on the corresponding Maurer-Cartan spaces, which isomorphic to  $H^1(L_p, \Lambda_+)$  due to the dimension reason,

$$\Phi : H^1(L_p, \Lambda_+) \rightarrow H^1(L_p, \Lambda_+), \quad (11)$$

a priori is not identity if  $L_{\phi(t)}$  bounds holomorphic discs of Maslov index zero for some  $t \in [0, 1]$  [20]. The following lemma states that  $\Phi$  only depends on the homotopy class of the path  $\phi$ .

**Lemma 4.1.** [44, Theorem 2.7]  $\Phi \equiv 1 \pmod{\Lambda_+}$  and  $\Phi$  only depends on the homotopy class of  $\phi$  assuming no appearance of negative Maslov index discs in the homotopy. In particular, if  $\phi$  is a contractible loop, then the corresponding  $\Phi = 1$  (before modulo  $\Lambda_+$ )<sup>6</sup>.

The explicit form of  $\Phi$  can be computed in the case of hyperKähler surfaces with assumptions and one can see that  $\Phi$  acts like wall crossing in the Gross-Siebert program in the theorem below.

**Theorem 4.2.** [40, Theorem 6.15] Let  $\gamma$  be a primitive relative class and assuming that  $k\gamma$  are the only relative classes such that  $L_{\phi(t)}$  bound holomorphic discs,  $k \in \mathbb{N}$ . Suppose that  $\text{Arg}Z_\gamma(u_-) < \text{Arg}Z_\gamma(u_+)$  (Check Remark 5.17 for the discussion of the signs). Then the transformation  $\Phi$  is given by

$$\mathcal{K}_\gamma : z^{\partial\gamma'} \mapsto z^{\partial\gamma'} f_\gamma^{\langle \gamma', \gamma \rangle}, \quad (12)$$

for some power series  $f_\gamma \in 1 + T^{\omega(\gamma)} z^{\partial\gamma} \mathbb{R}[[T^{\omega(\gamma)} z^{\partial\gamma}]]$ . Here  $\langle \gamma', \gamma \rangle$  denotes the intersection pairing of the corresponding boundary classes in the torus fibre.

The coefficients of  $\log f_\gamma$  have enumerative meanings: counting of the Maslov index zero discs bounded by the 1-parameter family of Lagrangians [37] or counting of rational curves with certain tangency conditions [23]. This motivates the following definition. More precisely, we define the open Gromov-Witten invariants  $\tilde{\Omega}(\gamma; u)$  below:

**Definition 4.3.** [40] With the notation as in Theorem 4.2 and  $u \in B_0$  is the intersection of image of  $\phi$  and  $l_\gamma$ . The open Gromov-Witten invariants  $\tilde{\Omega}(\gamma; u)$  are defined via the formula

$$\log f_\gamma = \sum_{d \in \mathbb{N}} d \tilde{\Omega}(d\gamma; u) (T^{\omega(\gamma)} z^{\partial\gamma})^d.$$

For other choices of  $(u, \gamma)$ , we set  $\tilde{\Omega}(\gamma; u) = 0$ . In other words,  $\tilde{\Omega}(\gamma; u) = 0$  only if  $\mathcal{M}_\gamma((X, J), L_u) \neq \emptyset$  from (10).

Then BPS rays are defined to be the support of loci with non-trivial open Gromov-Witten invariants of the same homology classes (up to parallel transport).

<sup>6</sup>Lemma 4.3.14 [20] showed that the homotopic  $A_\infty$ -homomorphisms induced the same map on the Maurer-Cartan spaces.

**Definition 4.4.** Given  $u \in B_0$  and a relative class  $\gamma \in H_2(X, L_u)$ , then the associated BPS ray is defined (locally) to be

$$l_\gamma := \{u' \in B_0 \mid \tilde{\Omega}(\gamma; u') \neq 0 \text{ and } Z_\gamma(u') \in \mathbb{R}_+\}.$$

Recall that the geometry  $X = X_*$  is not compact and a priori the moduli spaces of  $J$ -holomorphic discs may not be compact. However, from the curvature decay and injectivity radius decay in [30, Theorem 1.5] and the qualitative version of Gromov compactness theorem (see for instance [10, Proposition 5.3] or [22]), the moduli spaces of discs in  $X$  with compact Lagrangian boundary conditions are compact. To compute the open Gromov-Witten invariants on  $X$ , we first recall the following fact: Given a rational elliptic surfaces  $Y'$  and a fibre  $D'$ , there exists a 1-parameter deformation  $(Y_t, D_t)$  such that  $D'_t \cong D'$  and  $Y'_t$  rational elliptic surfaces with only type  $I_1$  singular fibres except  $D'_t$ . The following theorem explains how to compute the local open Gromov-Witten invariants near a general singular fibre other than those of type  $I_1$ . We will denote  $X_t$  to be the hyperKähler rotation of  $Y'_t \setminus D'_t$  with relation similar to (8). Then  $X_t \rightarrow B_t$  be a 1-parameter family of hyperKähler surfaces with special Lagrangian fibration and  $X_0 = X$ . We will identify  $B_t \cong B_0 = B$  topologically.

**Theorem 4.5.** [39, Theorem 4.3] Given any  $u \in B_0$ ,  $\gamma \in H_2(X, L_u)$ , then there exists  $t_0$  and a neighborhood  $\mathcal{U} \subseteq B_0$  of  $u$  such that

1. If  $\tilde{\Omega}(\gamma; u) = 0$ , then  $\tilde{\Omega}(\gamma; u') = 0$  for  $u' \in \mathcal{U}$ .
2. If  $\tilde{\Omega}(\gamma; u) \neq 0$ , then  $l_\gamma^t \cap \mathcal{U} \neq \emptyset$  and

$$\tilde{\Omega}_t(\gamma; u') = \tilde{\Omega}(\gamma; u),$$

for  $u' \in l_\gamma^t \cap \mathcal{U}$  and  $t$  with  $|t| < t_0$ .

Here  $\tilde{\Omega}_t(\gamma; u)$  denotes the open Gromov-Witten invariant of  $X_t$ .

For instance, in the case for the singular configuration of  $Y'$  is  $II^*II$ , then the BPS rays of  $X_t$  would look like the following picture with the notation defined in Section 5:

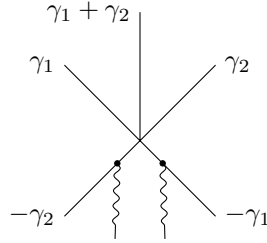


Figure 2: BPS rays on  $B_t$  for the case discussed in Section 5

## 4.2 Location of BPS Rays

In this section, we will restrict to the case  $Y'$  has exactly two singular fibres at  $0, \infty$  and the monodromy of the singular fibre is of finite order. The examples listed in Section 3 are exactly those possible  $Y'$ . We will show that the BPS rays divide the base into chambers which are one-to-one correspondence to the torus charts of the family Floer mirror later. In particular, the following observation simplifies the explicit computation of family Floer mirror.

**Lemma 4.6.** Let  $\gamma$  be one of the relative classes in Theorem 5.8. Then  $l_{\gamma_i}$  does not intersect each other. Specifically,  $B_0$  is divided into chambers by  $l_{\gamma_i}$ .

*Proof.* Let  $v \in TB$  and recall that one has  $vZ_\gamma = \int_{\partial_\gamma} \iota_{\tilde{v}} \Omega$ , where  $\tilde{v}$  is a lifting of  $v$ , by direct computation. Together with  $\Omega$  is holomorphic symplectic,  $Z_\gamma$  has no critical point in  $B_0$ . Let  $l_\gamma$  be a BPS ray, then by definition the holomorphic function  $Z_\gamma$  has phase 0 along  $l_\gamma$ . Now take  $v$  to be the tangent of  $l_\gamma$  at  $u \in l_\gamma$

pointing away from the origin. Therefore,  $vZ_\gamma(u) \neq 0$ . Otherwise,  $u$  is a critical point of  $Z_\gamma$  and contradicts to the fact that  $\Omega$  is holomorphic symplectic. In other words, the function  $|Z_\gamma|$  is strictly increasing along  $l_\gamma$ .

Next we claim that  $l_\gamma$  can not wrap inside a compact set. Otherwise, there exists a sequence of points  $u_i \in l_\gamma$  converging to some point  $u_\infty \in B_0$ . Since the monodromy is finite, there are only finitely possibly relative classes among  $\gamma_{u_i}$  with respect to the trivialization of the local system  $H_2(X, L_u)$  in a small neighborhood of  $u_\infty$ . Here  $\gamma_{u_i}$  is the parallel transport of  $\gamma$  to  $u_i$ . After passing to a subsequence, one has  $\lim_{i \rightarrow \infty} Z_\gamma(u_i) = Z_\gamma(u_\infty)$ . If  $u_\infty \in B_0$ , then  $l_\gamma$  can be extended over  $u_\infty$  and leads to a contradiction. Therefore,  $l_\gamma$  connects 0 and  $\infty$ . Then from the asymptotic geometry near infinity, one has  $|Z_\gamma| \nearrow \infty$  along  $l_\gamma$ .

Notice that the above argument holds for  $l_\gamma^\theta$ , where  $l_\gamma^\theta$  is the loci where  $Z_\gamma$  has phase  $\theta \in S^1$ . This implies that  $|Z_\gamma(u)|$  as  $u \rightarrow \infty$ . Recall that  $Z_\gamma(u)$  is a multi-valued holomorphic function on  $B_0 \cong \mathbb{C}^*$ . Since  $\pi_1(B_0) \cong \mathbb{Z}$  and the monodromy is of order  $k$ , we have  $Z_\gamma(u^k)$  is a well-defined holomorphic function  $\mathbb{C}^* \rightarrow \mathbb{C}^*$ . By straight-forward calculation one has  $\lim_{u \rightarrow 0} Z_\gamma(u^k) = 0$  and thus  $u = 0$  is a removable singularity. The previous discussion implies that  $\infty$  is a pole and the holomorphic function  $Z_\gamma(u^k)$  extends to  $\mathbb{P}^1 \rightarrow \mathbb{P}^1$  and fixing 0,  $\infty$ . Thus, we reach that

$$Z_\gamma(u^k) = cu, \quad (13)$$

for some constant  $c \in \mathbb{C}^*$  and the lemma follows.  $\square$

**Remark 4.7.** Let  $Y_t$  be a small deformation of  $Y$  such that  $Y_t$  has a fibre isomorphic to  $D$  and all other singular fibres are of type  $I_1$ , then the BPS rays still divide the base into five chambers.

**Remark 4.8.** Let  $Y$  be the del Pezzo surface of degree five and  $D$  be an anti-canonical divisor consists of a wheel of five rational curves. Set  $X = Y \setminus D$ . It is known that  $X$  is the moduli space of flat connections on punctured sphere [5]. There exists a hyperKähler metric on it such that suitable hyperKähler rotation becomes some meromorphic Hitchin moduli space, which is  $X'$ , the complement of the  $II^*$  fibre of the rational elliptic surface  $Y'$  with singular configuration  $II^*II$ . It is not clear if the holomorphic volume form  $\Omega'$  on  $X'$  extends as a meromorphic form with a simple pole along the  $II^*$  fibre. However, the Hitchin metric is exponentially asymptotic to the semi-flat metric at infinity [16], the proof of Lemma 4.6 also applies to this case.

### 4.3 Construction of the Family Floer Mirror

We will briefly recall the construction of family Floer mirror constructed by Tu [44] in this section. We will refer the details of the analytic geometry to [12].

**Definition 4.9.** Let  $U \subseteq B_0$  be an open set and  $\psi : U \rightarrow \mathbb{R}^n$  be the affine coordinate such that  $\psi(u) = 0$  for some  $u \in U$ . Then we say  $U$  is a rational domain if  $U \cong \psi(U) = P \subseteq \mathbb{R}^n$  is a rational convex polytope. The Tate algebra  $T_U$  associated to a rational domain  $U$  consists of the power series of the form

$$\sum_{\mathbf{k} \in \mathbb{Z}^n} a_{\mathbf{k}} z_1^{k_1} \cdots z_n^{k_n},$$

where  $\mathbf{k} = (k_1, \dots, k_n)$  with the following conditions:

1.  $a_{\mathbf{k}} \in \Lambda$  the Novikov field and
2. (convergence in  $T$ -adic topology)

$$\lim_{\mathbf{k} \rightarrow \infty} \text{val}(a_{\mathbf{k}}) + \langle \mathbf{k}, \mathbf{x} \rangle \rightarrow \infty, \quad (14)$$

as  $\mathbf{k} \rightarrow \infty$ , for each  $\mathbf{x} = (x_1, \dots, x_n) \in U$ .

For such rational domain  $U$ , we denote  $\mathcal{U}$  be the maximum spectrum of the associated Tate algebra  $T_U$ .

**Remark 4.10.** Recall that the Novikov field  $\Lambda$  is algebraically closed. From Proposition 3.18 (c) [13],  $\mathcal{U}$  is identified with  $\text{Val}^{-1}(\psi(U))$ , where  $\text{Val} : (\Lambda^*)^n \rightarrow \mathbb{R}^n$  is component-wise the valuation on  $\Lambda^*$ . If  $f \in T_U$ , then  $f(x)$  converges for all points  $x \in \mathcal{U}$  and thus we may view  $f$  as a function defined on  $\text{Val}^{-1}(\psi(U))$ .

Take an open cover of rational domains  $\{U_i\}_{i \in I}$  of  $B_0$  with affine coordinates  $\psi_i : U_i \rightarrow \mathbb{R}^n$  such that  $\psi_i(u_i) = 0 \in \mathbb{R}^n$  for some  $u_i \in U_i$ . For each pair  $i, j$  with  $U_i \cap U_j \neq \emptyset$ , there is a natural gluing data

$$\Psi_{ij} : \mathcal{U}_i \rightarrow \mathcal{U}_j,$$

which now we will explain below: Choose  $p \in U_i \cap U_j$  and  $f_{u_i, p}$  fibrewise preserving diffeomorphism sending  $L_{u_i}$  to  $L_p$  and is identity outside  $U_i$ . Let  $(x_1^i, \dots, x_n^i)$  (and  $(x_1^j, \dots, x_n^j)$ ) be the local symplectic affine coordinates on  $U_i$  (and  $U_j$  respectively) with respect to the same set of basis up to parallel transport within  $U_i, U_j$ . The corresponding functions in  $T_{U_i}$  are denoted by  $(z_1^i, \dots, z_n^i)$ , where  $\text{val}(z_k^i) = x_k^i$ .

The difference of symplectic affine coordinates is

$$\int_{f_{u_i, p}^* \beta} \omega - \int_{\beta} \omega = \left\langle \sum_{k=1}^n (x_k(p) - x_k(u_i)) e_k^i, \partial \beta \right\rangle.$$

Denote  $T_{U_i, p}$  the Tate algebra satisfying the convergence in  $T$ -adic topology (14) on the rational domain  $\phi_i(U_i) - \phi_i(p)$  and  $\mathcal{U}_{i, p}$  as its spectrum. Then there is the transition map

$$\begin{aligned} S_{u_i, p} : \mathcal{U}_i &\rightarrow \mathcal{U}_{i, p} \\ z_k^i &\mapsto T^{x_k(u_i) - x_k(p)} z_k^i. \end{aligned} \quad (15)$$

Then define the gluing data  $\Psi_{ij}$  be the composition

$$\Psi_{ij} : \mathcal{U}_{ij} \xrightarrow{S_{u_i, p}} \mathcal{U}_{ij, p} \xrightarrow{\Phi_{ij}} \mathcal{U}_{ji, p} \xrightarrow{S_{u_j, p}^{-1}} \mathcal{U}_{ji}, \quad (16)$$

where  $\Phi_{ij}$  is defined in (11). The gluing data  $\Psi_{ij}$  satisfies (Section 4.9 [44])

1. Independent of the choice of reference point  $p \in U_i \cap U_j$ .
2.  $\Psi_{ij} = \Psi_{ji}$  and  $\Psi_{ij} \Psi_{jk} = \Psi_{ik}$ .
3. For  $p \in U_i \cap U_j \cap U_k$ , we have  $\Psi_{ij}(\mathcal{U}_{ij} \cap \mathcal{U}_{ik}) \subseteq \mathcal{U}_{ji} \cap \mathcal{U}_{jk}$ .

Then the family Floer mirror  $\check{X}$  is defined to be the gluing of the affinoid domains

$$\check{X} := \bigcup_{i \in I} \mathcal{U}_i / \sim, \quad (17)$$

where  $\sim$  is defined by (16). The natural projection map  $T_U \rightarrow U$  from the valuation glue together and gives the family Floer mirror a projection map

$$\mathfrak{Trop} : \check{X} \rightarrow B_0.$$

The following example is straight forward from the construction.

**Example 4.11.** Recall that the rigid analytic torus  $(\mathbb{G}_m^{an})^2$  admits a valuation map  $\mathfrak{Trop} : (\mathbb{G}_m^{an})^2 \rightarrow \mathbb{R}^2$ . Let  $\pi : X \rightarrow U$  be a Lagrangian fibration such that for any path  $\phi$  connecting  $u_i, u_j \in U$ , the corresponding  $F_\phi = id$ . Assume that the symplectic affine coordinates give an embedding  $U \rightarrow \mathbb{R}^2$  and we will simply identify  $U$  with its image. Then the gluing

$$\begin{aligned} \Psi_{ij} : \mathcal{U}_{ij} &\rightarrow \mathcal{U}_{ji} \\ z_k^i &\mapsto T^{x_k(u_i) - x_k(u_j)} z_k^j, \end{aligned}$$

is simply translation from equation (16). Thus the corresponding family mirror  $\check{X}$  is simply  $\mathfrak{Trop}^{-1}(U) \rightarrow U$ . In particular, when  $U \cong \mathbb{R}^2$ , then the family Floer mirror is simply the rigid analytic torus  $(\mathbb{G}_m^{an})^2$ . It worth noticing that if  $U \subseteq \mathbb{R}^2$  is a proper subset, then  $\mathfrak{Trop}^{-1}(U)$  is not a dense subset of  $(\mathbb{G}_m^{an})^2$ .

## 5 Family Floer Mirror of $X_{II}$

In this section, we will have a detailed computation of the family Floer mirror of  $X = X_{II}$  (see Section 3). We sketch the proof below: We will first identify the locus of special Lagrangian fibres bounding holomorphic discs to be simply five rays  $l_{\gamma_i}$  connecting  $0, \infty$ . Then we compute their corresponding wall-crossing transformations which are analytification of some birational maps. Thus, the family Floer mirror  $\check{X}$  can be glue from five charts. Then we will prove that the embedding of each of the five charts into  $\check{X}$  can be extended to an embedding of the analytic torus  $\mathbb{G}_m^{an}$  into  $\check{X}$ . In other words,  $\check{X}$  is gluing five analytic torus. On the other hand, consider the del Pezzo surface  $Y$  of degree 5 and  $D$  be the cycle of five rational curves. Let  $B_{\text{GHK}}$  be the affine manifold with the singularity constructed in Section 2.1 after choosing suitable branch cut. We identify the complex affine structure on  $B$  with the one on  $B_{\text{GHK}}$ , the rays and the corresponding wall-crossing transformations. Then from [24, Example 3.7], we know that  $\check{X}$  is the analytification of the del Pezzo surface of degree five. Furthermore, we would choose the branch cuts on  $B$  in a different way. This would induce another realization of  $\check{X}$  as gluing to five tori but with different gluing morphisms, which we will later identify  $\check{X}$  as the  $\mathcal{X}$ -cluster variety of type  $A_2$ .

As discussed in Section 3, the base  $B$  with the complex structure from the elliptic fibration  $Y'_{II} \rightarrow \mathbb{P}^1$  is biholomorphic to  $\mathbb{C}$  as a subset of  $\mathbb{P}^1$ . We may choose a holomorphic coordinate  $u$  on  $B$  such that the fibres over  $u = 0, \infty$  are the type  $II, II^*$  singular fibres. Such coordinate is unique up to scaling  $\mathbb{C}^*$ . We will determine such scaling later. First we apply Theorem 4.5 to the 1-parameter family of hyperKähler rotation of the rational elliptic surfaces described in Section 3, one get

**Theorem 5.1.** [39, Theorem 4.11] *Choose a branch cut from the singularity to infinity and a basis  $\{\gamma'_1, \gamma'_2\}$  of  $H_2(X, L_u) \cong \mathbb{Z}^2$  such that  $\langle \gamma'_1, \gamma'_2 \rangle = 1$  and the counter-clockwise monodromy  $M$  around the singularity is*

$$\begin{aligned} \gamma'_1 &\mapsto -\gamma'_2 \\ \gamma'_2 &\mapsto \gamma'_1 + \gamma'_2 \end{aligned} \tag{18}$$

with respect to the basis. Then for  $|u| \ll 1$ , one has

$$\tilde{\Omega}(\gamma; u) = \begin{cases} \frac{(-1)^{d-1}}{d^2}, & \text{if } \gamma = \pm d\gamma'_1, \pm d\gamma'_2, \pm d(\gamma'_1 + \gamma'_2), \text{ for } d \in \mathbb{N} \\ 0, & \text{otherwise.} \end{cases}$$

**Remark 5.2.** See Remark 2.10 [39] for the relation between  $\tilde{\Omega}(\gamma; u)$  and  $\Omega(\gamma; u)$  in the reference.

**Remark 5.3.** The monodromy (18) acts transitively on the set  $\{\pm\gamma'_1, \pm\gamma'_2, \pm(\gamma'_1 + \gamma'_2)\}$ .

**Remark 5.4.** If  $A \in GL(2, \mathbb{Z})$  such that  $A \begin{pmatrix} 0 & -1 \\ 1 & 1 \end{pmatrix} = \begin{pmatrix} 0 & -1 \\ 1 & 1 \end{pmatrix} A$ , then  $A = \begin{pmatrix} 0 & -1 \\ 1 & 1 \end{pmatrix}^k$  for some  $k \in \mathbb{N}$ .

Therefore, if  $\gamma_1, \gamma_2 \in H_2(X, L_u)$  such that the monodromy is the form of (18), then  $\gamma_1 = M^k \gamma'_1, \gamma_2 = M^k \gamma'_2$  for some  $k \in \mathbb{N}$ .

Furthermore, we will next show that these are the only possible relative classes with non-trivial open Gromov-Witten invariants even **globally** in  $X_{II}$ .

**Corollary 5.5.** *If  $\tilde{\Omega}(\gamma; u) \neq 0$ , then  $\gamma$  is one of the relative classes in Theorem 5.1,  $u \in l_\gamma$  and  $\tilde{\Omega}(\gamma; u) = \frac{(-1)^{d-1}}{d^2}$ , where  $d$  is the divisibility of  $\gamma$ .*

*Proof.* This is a direct consequence of the split attractor flow mechanism of the open Gromov-Witten invariants  $\tilde{\Omega}(\gamma; u)$  (see [40, Theorem 6.32]). We will sketch the proof here for self-containedness. Let  $l_\gamma$  be a ray emanating from  $u$  such  $\omega_\gamma$  is decreasing along  $l_\gamma$ . From Gromov compactness theorem, the loci where  $\tilde{\Omega}(\gamma)$  jumps are discrete. Assume that  $\tilde{\Omega}(\gamma)$  is invariant along  $l_\gamma$ , then the holomorphic disc representing  $\gamma$  can only fall into a tubular neighborhood of the singular fibre over 0 by [10, Proposition 5.3] when the symplectic area decrease to small enough. Therefore by Lemma 5.1,  $\gamma$  is one of the relative classes in Theorem 5.1. Otherwise, assume  $u_1$  is the first point where  $\tilde{\Omega}(\gamma)$  jumps. Apply Lemma 4.1 to a small loop around  $u_1$ , there exists  $\gamma_\alpha, \alpha \in A$  such that  $\tilde{\Omega}(\gamma_\alpha; u_1) \neq 0$  and  $\gamma = \sum_{\alpha \in A} \gamma_\alpha$ . In particular,  $\omega(\gamma_\alpha) < \omega(\gamma)$ . One may replace  $(\gamma, u)$  by  $(\gamma_\alpha, u_1)$  and run the procedure. Again by Gromov compactness theorem, after finitely many

splittings, all the relative classes are among the one listed in Theorem 5.1. To sum up, there exists a rooted tree  $T$  and a continuous map  $f$  such that the root maps to  $u$ , each edge is mapped to an affine line segment and all the 1-valent vertex are mapped to 0. Since the affine line corresponding to the relative classes in Theorem 5.1 do not intersect by Lemma 4.6, the lemma follows.  $\square$

Although there are six classes of relative classes support non-trivial open Gromov-Witten invariants, next we explain that there are actually only five BPS rays emanating from  $u = 0$  due to the monodromy.

Thanks to Remark 5.3, we will choose the scaling of the coordinate  $u$  such that the branch cut is  $\text{Arg}(u) = 0^-$  and  $l_{\gamma_1} = \{u \in \mathbb{R}_+\}$ , where  $\gamma_1 = -\gamma'_1$ . Denote  $\gamma_{i+1} = M\gamma_i$  on the complement of branch cut, for  $i \in \mathbb{Z}$ . Straight-forward calculation shows that  $\gamma_{i+6} = \gamma_i$  and  $\gamma_{i-1} - \gamma_i + \gamma_{i+1} = 0$ . Denote the symplectic and complex affine coordinate (with respect to  $\gamma_k, \gamma_{k+1}$ ) discussed in Section 3.1 by

$$x_k = \int_{\gamma_k} \omega, \quad y_k = \int_{\gamma_{k+1}} \omega \quad (19)$$

$$\tilde{x}_k = \int_{\gamma_k} \text{Im}\Omega, \quad \tilde{y}_k = \int_{\gamma_{k+1}} \text{Im}\Omega. \quad (20)$$

We will also denote

$$\begin{aligned} x &= \int_{-\gamma'_1} \omega, & y &= \int_{\gamma'_2} \omega, \\ \tilde{x} &= \int_{\gamma'_2} \text{Im}\Omega, & \tilde{y} &= \int_{-\gamma'_1} \text{Im}\Omega, \end{aligned} \quad (21)$$

which give another set of symplectic/complex affine coordinates.

Recall that  $x_k(u) - i\tilde{x}_k(u) = Z_{\gamma_k}(u)$  is a holomorphic function with respect to the above complex structure on  $B$  defined on the complement of the branch cut and can be analytic continued to a multi-valued holomorphic function on  $\mathbb{C}^*$ . In particular, if  $\gamma$  is a relative class in Theorem 5.1, then  $x_k(u) > 0$  and  $\tilde{x}_k(u) = 0$  along a BPS ray  $l_{\gamma_k}$ . From (13), one have

$$x_k - i\tilde{x}_k = c_k u^{\frac{a}{6}}, \quad k \in \mathbb{Z}, \quad (22)$$

for some constant  $a \in \mathbb{N}, c_k \in \mathbb{C}^*$ . With more analysis, we have the following lemma

**Lemma 5.6.** *With the above choice of coordinate  $u$  on  $B_0 \cong \mathbb{C}^*$ , we have*

$$x_k - i\tilde{x}_k = e^{2\pi i(k-1)\frac{5}{6}} u^{\frac{5}{6}}. \quad (23)$$

*In particular, the angle between  $l_{\gamma_k}$  and  $l_{\gamma_{k+1}}$  is  $\frac{2\pi}{5}$  with respect to the conformal structure after hyperKähler rotation <sup>7</sup>.*

*Proof.* From the normalization, we have  $x_1 - i\tilde{x}_1 = u^{\frac{a}{6}}$ . Recall that  $Z_{\gamma_k} := x_k - i\tilde{x}_k$ . From the monodromy  $M\gamma_k = \gamma_{k+1}$ , we have

$$Z_{\gamma_{k+1}}(u) = Z_{\gamma_k}(ue^{2\pi i}) = e^{2\pi i\frac{a}{6}} Z_{\gamma_k}(u).$$

Here recall that  $Z_{\gamma_i}(u)$  is a priori only defined on the complement of the branch cut and we use  $Z_{\gamma}(ue^{2\pi i})$  to denote the value of analytic continuation across the branch cut counter-clockwise once at  $u$ .

Now it suffices to show that  $a = 5$  or show that  $Z_{\gamma_i}(u) = O(|u^{\frac{5}{6}}|)$ . This can be seen by direct computation. Indeed, for  $u$  close enough to the origin  $0 \in B$ , the representatives of  $\gamma_i$  can be chosen to be in a neighborhood of the singular point of the type  $II$  singular fibre. In such neighborhood,  $X'_{II}$  is defined by  $y^2 = x^3 + u$ . One can write  $\Omega' = \frac{2f(u)}{u} dy \wedge dx = f(u) du \wedge \frac{dx}{y}$ <sup>8</sup> for some holomorphic function  $f(u)$  with  $f(0) \neq 0$ , since  $\Omega'$  is a non-vanishing holomorphic 2-form on  $X'_{II}$ . Consider the 2-chain  $\gamma_{i,j}, i \neq j$ , which is an  $S^1$ -fibration

<sup>7</sup>Notice that there is no well-defined notion of angle with only an affine structure on  $B_0$  and thus one does not see this aspect on the affine manifold used in Gross-Hacking-Keel.

<sup>8</sup>Notice that  $u = y^2 - x^3$  is a well-defined function on the chart.

over a line segment from  $u = 0$  to  $u = u_0$ . The fibre over  $u$  is topologically the compactification of  $y^2 = x^3 + u$  and the  $S^1$  is the double cover of path connecting  $\zeta^i(-u)^{\frac{1}{3}}, \zeta^j(-u)^{\frac{1}{3}}$  in  $x$ -plane, where  $\zeta = \exp(2\pi i/3)$ . Each of  $\gamma_{i,j}$  can be represented by the 2-chain parametrized by  $u = tu_0$ ,  $x = s\zeta^i(-u)^{\frac{1}{3}} + (1-s)\zeta^j(-u)^{\frac{1}{3}}$ , with  $t \in [0, 1], s \in [0, 1]$ . Since  $\partial\gamma_i$  are vanishing cycles,  $\gamma_i$  can be represented by some linear combination  $a\gamma_{0,1} + b\gamma_{1,2}$  with  $a, b \in \mathbb{Z}$  and  $a^2 + b^2 \neq 0$ .

Then by direct calculation, one has

$$\begin{aligned}
Z_{\gamma_{i,j}}(u_0) &= \int_{\gamma_{i,j}} \Omega' = \int_{u=0}^{u=u_0} \int_{x=\zeta^i(-u)^{\frac{1}{3}}}^{x=\zeta^j(-u)^{\frac{1}{3}}} f(u) du \wedge \frac{dx}{y} \\
&= \int_{u=0}^{u=u_0} \left( \int_{x=\zeta^i(-u)^{\frac{1}{3}}}^{x=\zeta^j(-u)^{\frac{1}{3}}} \frac{dx}{y} \right) du + O(|u_0|) \\
&= \int_{u=0}^{u=u_0} \left( \int_{x=\zeta^i(-u)^{\frac{1}{3}}}^{x=\zeta^j(-u)^{\frac{1}{3}}} \frac{dx}{(x^3 + u)^{\frac{1}{2}}} \right) du + O(|u_0|) \\
&= \int_{u=0}^{u=u_0} \left( \int_{s=0}^{s=1} \frac{x'(s) ds}{((x(s) - \zeta^i(-u)^{\frac{1}{3}})(x(s) - \zeta^j(-u)^{\frac{1}{3}})(x(s) - \zeta^k(-u)^{\frac{1}{3}}))^{\frac{1}{2}}} \right) du + O(|u_0|).
\end{aligned} \tag{24}$$

$$\tag{25}$$

Here we have  $k \in \{0, 1, 2\} \setminus \{i, j\}$  and we use the change of variable  $x(s) = s\zeta^i(-u)^{\frac{1}{3}} + (1-s)\zeta^j(-u)^{\frac{1}{3}}$  in the forth line. Using  $x'(s) = O(u^{\frac{1}{3}})$  and factoring out  $u^{\frac{1}{2}}$  in the denominator of the last line of (24), we have the part in the parenthesis is asymptotic to  $\frac{u^{\frac{1}{3}}}{u^{\frac{1}{2}}} \int_0^1 \frac{ds}{((s(1-s))^{\frac{1}{2}})} = O(u^{-\frac{1}{6}})$ . From the fact that  $\int_0^{u_0} u^{-\frac{1}{6}} du = O(u_0^{\frac{5}{6}})$ , we arrive at

$$Z_{\gamma_{i,j}}(u) = C_{i,j} u^{\frac{5}{6}} + O(|u|),$$

where  $C_{i,j}$  is some constant independent of  $u_0$  and  $C_{0,1}, C_{1,2}$  is linear independent over  $\mathbb{Z}$ . Thus, we have similar estimate

$$Z_{\gamma_i}(u) = O(u^{\frac{5}{6}}).$$

In particular, it implies that  $Z_{\gamma_1}(u) = u^{\frac{5}{6}}$  from the choice of the normalization of  $u$ . Then

$$Z_{\gamma_2}(u) = Z_{M\gamma_1}(u) = (e^{2\pi i} u)^{\frac{5}{6}} = e^{2\pi i \frac{5}{6}} u^{\frac{5}{6}}.$$

Thus,  $Z_{\gamma_2}(u) \in \mathbb{R}_{>0}$  if and only if  $u \in \mathbb{R}_{>0} e^{\frac{2\pi i}{5}}$ . On the other hand, when  $u \in l_{\gamma_k}$ , one has  $Z_{\gamma_k}(u) = \int_{\gamma_k} \omega - i \int_{\gamma_k} \text{Im} \Omega \in \mathbb{R}_{>0}$  by Remark 3.3 and the fact that symplectic area is of a holomorphic disc is positive. Thus, we have  $l_{\gamma_2} = \{u \in \mathbb{R}_{>0} e^{\frac{2\pi i}{5}}\}$ , or the angle between  $l_{\gamma_1}, l_{\gamma_2}$  is  $\frac{2\pi}{5}$ . The general statement of the second part of the lemma can be then proved inductively.  $\square$

**Remark 5.7.** With Lemma 5.6, one can see that  $Z_{\gamma_6} \notin \mathbb{R}_+$  until  $u$  varies across the branch cut counter-clockwisely. If one analytic continues  $Z_{\gamma_6}$  across the branch cut counter-clockwisely becomes  $Z_{\gamma_7} = Z_{\gamma_1}$  because  $\gamma_7 = M\gamma_6$  and  $M^6 = \text{id}$ . Therefore, the corresponding BPS ray is again has the same locus as  $l_{\gamma_1}$ . In particular, there are only five BPS rays in total. In other words, there are only five families of discs with non-trivial open Gromov-Witten invariant and contribute to the construction of the family Floer mirror.

We conclude the above discussion now:

**Theorem 5.8.** With the notation above,

$$\gamma_1 = -\gamma'_1, \gamma_2 = \gamma'_2, \gamma_3 = \gamma'_1 + \gamma'_2, \gamma_4 = \gamma'_1, \gamma_5 = -\gamma'_2.$$

Then



1.  $f_\gamma(u) \neq 1$  if and only if  $u \in l_{\gamma_i}$  and  $\gamma = \gamma_i$  for some  $i = 1, \dots, 5$ .
2. In such cases,  $f_{\gamma_i} = 1 + T^{\omega(\gamma_i)} z^{\partial \gamma_i}$ .
3. The branch cut can be chosen to be between  $l_{\gamma_1}$  and  $l_{\gamma_5}$ .

*Proof.* Remark 5.7 explains that there are actually five BPS rays  $l_{\gamma_i}, i = 1, \dots, 5$ . The second statement comes from Definition 4.3 and Theorem 5.1. The third statement is how we define the branch cut below Corollary 5.5.  $\square$

The affine structure is illustrated in Figure 3. In Figure 3, the curvy ray, between  $l_{\gamma_5}$  and  $l_{\gamma_1}$ , represents the branch cut. The ‘monodromy’ of the affine structure, can be seen as gluing the the curvy ray with  $l_{\gamma_1}$ . The shaded region denoted where the gluing is.

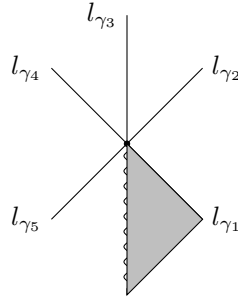


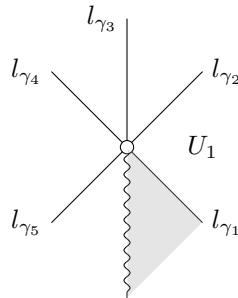
Figure 3: BPS rays near the singularity.

Straight-forward calculation shows that

$$\gamma_{i+2} = -\gamma_i + \gamma_{i+1}, \quad (26)$$

which is the analogue of (1).

### 5.1 Construction of Family Floer Mirror of $X_{II}$



Let  $U_k$  be the chamber bounded by  $l_{\gamma_k}$  and  $l_{\gamma_{k+1}}$  in  $B_0$ ,  $i = 1, \dots, 4$  and  $U_5$  be the chamber bounded by  $l_{\gamma_5}$  and  $l_{\gamma_1}$ . Thus there are only 5 chambers. Recall that the dotted line represents a branch cut between  $l_{\gamma_1}$  and  $l_{\gamma_5}$ . With such branch cut and monodromy, we trivialized the local system  $H_2(X, L_u)$  over the complement of the branch cut. Recall that we have  $M\gamma_i = \gamma_{i+1}$  by definition.

Next, we compare the affine structure from the SYZ fibration with the one from Gross-Hacking-Keel (see Section 2.1).

**Lemma 5.9.** *The complex affine structure on  $B_0$  coincides with the affine manifold  $B_{\text{GHK}}$  with singularity constructed from del Pezzo surface of degree five relative to a cycle of five rational curves in [24].*

*Proof.* First notice that one can compute the complex affine coordinates on  $l_{\gamma_1}, l_{\gamma_2}$ ,

$$\begin{aligned} l_{\gamma_1} &= \{\check{y} = 0, \check{x} > 0\} \\ l_{\gamma_2} &= \{\check{x} = 0, \check{y} > 0\}. \end{aligned} \tag{27}$$

Indeed, we have  $\check{y} = 0$  on  $l_{\gamma_1}$  by Remark 3.3. From Lemma 5.6, we have

$$\check{x}(u) = \int_{\gamma'_2} \text{Im} \Omega = \text{Re} Z_{\gamma}(u) = \text{Re} Z_{-M\gamma'_1}(u) = -\text{Re}(ue^{2\pi i})^{\frac{5}{6}} > 0,$$

for  $u \in l_{\gamma_1}$ . One can compute the case of  $u \in l_{\gamma_2}$  similarly. Therefore, with respect to the complex affine structure, the primitive tangent vectors of  $l_{\gamma_1}, l_{\gamma_2}$  are given by  $\frac{\partial}{\partial \check{x}}, \frac{\partial}{\partial \check{y}}$ . To compare with the affine structure from Gross-Hacking Keel, we will identify them with  $\mathbb{R}_{>0}(1, 0), \mathbb{R}_{>0}(0, 1)$ . Then  $(-1, 1), (-1, 0), (0, -1)$  are the tangents of  $l_{\gamma_3}, l_{\gamma_4}, l_{\gamma_5}$  respectively by Lemma 5.6 and the relation  $-Z_{\gamma_i} + Z_{\gamma_{i+1}} = Z_{\gamma_{i+2}}$  which is the analogue of (1). Therefore, the complex affine coordinates on the region in  $\{u \in B_0 | 0 < \text{Arg} u < \frac{8\pi}{5}\}$  is isomorphic to the one on the sector (without the vertex) from  $(1, 0)$  counter-clockwise to  $(0, -1)$  viewed as an affine submanifold of  $\mathbb{R}^2$ . To understand the monodromy of the complex affine structure on  $B_0$ , one need to do the similar calculation across the branch cut. Consider the complex affine structure on the universal cover of  $B_0$ <sup>9</sup>. Then similar calculation shows that the complex affine coordinates on the region in  $\{u \in B_0 | 0 < \text{Arg}(u) < 2\pi\}$  is isomorphic to the one on the sector (without the vertex) from  $(1, 0)$  counter-clockwise to  $(-1, -1)$ , which denoted as  $\mathcal{V}_1$ , viewed as an affine submanifold of  $\mathbb{R}^2$ . If one change the location of the branch cut to  $\text{Arg}(u) = -\frac{2\pi}{5}^-$ , the complex affine structure on the region in  $\{u \in B_0 | -\frac{2\pi}{5} < \text{Arg} u < \frac{8\pi}{5}\}$  is isomorphic to the one on the sector (without the vertex) from  $(-1, -1)$  counter-clockwise to  $(0, -1)$ , denoted as  $\mathcal{V}_2$ , viewed as an affine submanifold of  $\mathbb{R}^2$ <sup>10</sup>. The affine coordinates on  $\{u \in B_0 | 0 < \text{Arg}(u) < \frac{8\pi}{5}\}$  from pull-back from  $\mathcal{V}_1, \mathcal{V}_2$  coincide, so the complex affine structure on  $\{-\frac{2\pi}{5} < \text{Arg}(u) < 2\pi\}$  (viewed as a subset of universal cover of  $B_0$ ) is isomorphic to the natural affine structure on  $\mathcal{V}_1 \cup \mathcal{V}_2$  as a subset of  $\mathbb{R}^2$ . Recall that set-wise  $l_{\gamma_6} = l_{\gamma_1}$  and  $l_{\gamma_5} = l_{\gamma_0}$  from Remark 5.7. Therefore,  $B_0$  as an affine manifold is simply the gluing of the sector bounded by  $(0, -1), (-1, -1)$  in  $\mathcal{V}_1$  and the sector bounded by  $(-1, -1), (1, 0)$  in  $\mathcal{V}_2$  linearly, which is exactly the description of  $B_{GHK}$ . Moreover, one sees that  $\{U_i\}_{i=1, \dots, 5}$  coincides with the decomposition  $\Sigma$  in Section 2.1.  $\square$

**Remark 5.10.** Write  $\check{x}'(u) = \check{x}(ue^{2\pi i}), \check{y}'(u) = \check{y}(ue^{2\pi i})$  as the continuation of  $\check{x}, \check{y}$  counterclockwisely. From (18)(21), one has

$$\begin{aligned} d\check{x}' &= d\check{x} - d\check{y} \\ d\check{y}' &= d\check{x} \end{aligned}$$

or equivalently

$$\begin{aligned} d\check{x} &= d\check{y}' \\ d\check{y} &= -d\check{x}' + d\check{y}'. \end{aligned}$$

Dually, the monodromy on the complex affine coordinate is given by

$$\begin{aligned} \frac{\partial}{\partial \check{x}'} &= \frac{\partial}{\partial \check{x}} + \frac{\partial}{\partial \check{y}} \\ \frac{\partial}{\partial \check{y}'} &= -\frac{\partial}{\partial \check{x}}, \end{aligned}$$

which exactly the gluing at the end of Lemma 5.9, sending  $(-1, 0)$  (and  $(-1, -1)$ ) to  $(-1, -1)$  (and  $(-1, 0)$  respectively).

<sup>9</sup>By abuse of notation, we still use the coordinate  $u$  for the corresponding holomorphic coordinate and  $\check{x}, \check{y}$  for the pull back of the complex affine structure.

<sup>10</sup>Alternatively, one may extend the affine structure across the original branch cut clock-wisely and then  $(-1, -1)$  is the primitive tangent of  $l_{\gamma_0}$ .

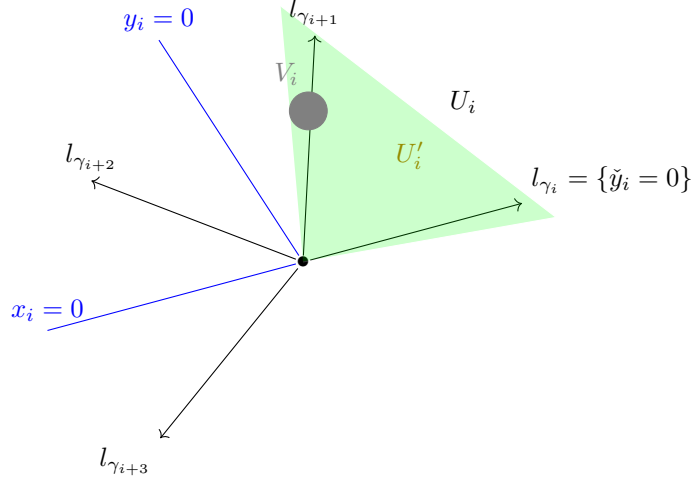


Figure 4: Illustration for the notations in the beginning of Section 5.1.

Notice that a priori  $l_{\gamma_i}$  is only an affine line with respect to the complex affine coordinates. To compute the family Floer mirror, we need to have a better control of the BPS rays in terms of the symplectic affine structure. The following observation comes from (22) directly.

**Lemma 5.11.** *Any ray with a constant phase is affine with respect to the symplectic affine structure. In particular,  $l_{\gamma_i}$  is an affine line with respect to the symplectic affine structure.*

*Proof.* Any such ray can be parametrized by  $z = Ct$  for some complex number  $C$ . From (22), the symplectic coordinates along the ray are given by  $x_k = C'_k t^{\frac{2\pi k}{5}}, y_k = C''_k t^{\frac{2\pi k}{5}}$ , for some  $C'_k, C''_k \in \mathbb{R}$  and the lemma follows. In other words, such ray is given by the affine line  $C'_k x_k = C''_k y_k$  with respect to the symplectic affine coordinates  $(x_k, y_k)$ .  $\square$

Recall that the family mirror  $\check{X}$  is defined by  $\coprod \mathcal{U}_\alpha / \sim$ , where  $\mathcal{U}_\alpha$  is the maximum spectrum of  $T_{U_\alpha}$ , for refined enough (so that the Fukaya trick applies) open covering  $\{U_\alpha\}_{\alpha \in A}$  and together with symplectic affine coordinates  $\psi_\alpha : U_\alpha \rightarrow \mathbb{R}^2$  such that  $\psi_\alpha(u_\alpha) = 0$  for some  $u_\alpha \in U_\alpha$ . We may take

$$\psi_\alpha(u) = (x(u) - x(u_\alpha), y(u) - y(u_\alpha)).$$

11

**Remark 5.12.** *On one hand, from Remark 4.10, we have  $\mathcal{U}_\alpha$  is identified with  $\text{Val}^{-1}(\psi_\alpha(U)) \subseteq (\Lambda^*)^2$ . On the other hand, from Example 4.11 and Theorem 5.8, if  $U_\alpha \subseteq U_k$  for any  $k \in 1, \dots, 5$ , then  $\mathcal{U}_\alpha \cong \mathfrak{Trop}^{-1}(U_\alpha)$ . Here we use the symplectic affine coordinates  $x, y$  on  $U_\alpha$  to embed  $U_\alpha$  into  $\mathbb{R}^2$  as an affine submanifold and  $\mathfrak{Trop} : (\mathbb{G}_{an}^2) \rightarrow \mathbb{R}^2$ . Recall that there is a natural identification  $(\Lambda^*)^2 \cong (\mathbb{G}_m^{an})^2$  as sets such that the below diagram commutes.*

$$\begin{array}{ccc} (\Lambda^*)^2 & \longrightarrow & (\mathbb{G}_m^{an})^2 \\ \text{Val} \searrow & & \swarrow \mathfrak{Trop} \\ & \mathbb{R}^2 & \end{array} \quad (28)$$

The two description of  $\mathcal{U}_\alpha$  simply differs by a translation

$$\begin{aligned} \text{Val}^{-1}(U_\alpha) &\rightarrow \mathfrak{Trop}^{-1}(U_\alpha) \\ (z_1, z_2) &\mapsto (T^{x(u_\alpha)} z_1, T^{y(u_\alpha)} z_2) \end{aligned}$$

under the above identification.

<sup>11</sup>Here we abuse the notation, denote  $x, y$  to be the natural extension of clock-wisely across the branch cut if  $U_\alpha$  intersects the branch cut and  $u \in U_5$ . In other words, one should replace  $(x, y)$  by  $(y, x - y)$  under the circumstances from (18).

Let  $\mathfrak{Trop}_i : (\mathbb{G}_m^{an})_i^2 \rightarrow \mathbb{R}_i^2$  be the standard valuation map. Here we put an subindex  $i$  for each analytic tori and later it would correspond to the five different tori. Now if  $U_\alpha \subseteq U_i$  for some  $i = 1, \dots, 5$  and  $U_\alpha \cap U_{\alpha'} \neq \emptyset$  with the reference  $u_{\alpha'} \in U_{i+1}$ , then again from Ex 4.11 and Theorem 5.8, one can naturally identify  $\mathcal{U}_\alpha \amalg \mathcal{U}_{\alpha'} / \sim \cong \mathfrak{Trop}^{-1}(U_\alpha \cup U_{\alpha'})$ . From the identification in Remark 5.12, the function  $T^{\omega(\gamma_{u_\alpha})} z^{\partial\gamma} \in T_{U_\alpha}$  and  $T^{\omega(\gamma_{u_{\alpha'}})} z^{\partial\gamma} \in T_{U_{\alpha'}}$  glue to a function on  $\mathfrak{Trop}^{-1}(U_\alpha \cup U_{\alpha'})$ , which is simply the restriction of  $z^{\partial\gamma}$  on  $(\Lambda^*)^2 \cong (\mathbb{G}_m^{an})^2$ .

Denote  $U'_i = \cup_\alpha U_\alpha$ , where  $\alpha$  runs through those  $u_\alpha \in U_i$ . By taking refinement of the open cover, we may assume that  $U_i \subseteq U'_i$  without loss of generality. Then we have the extension of the embedding  $\mathfrak{Trop}^{-1}(U_i) \subseteq \check{X}$  to  $\mathfrak{Trop}^{-1}(U'_i) \subseteq \check{X}$ . From the previous discussion, the family Floer mirror is simply  $\amalg_{i=1}^5 \mathfrak{Trop}_i^{-1}(U'_i) / \sim$ . Note that

$$\begin{aligned} \check{X} = \bigcup_i \mathfrak{Trop}_i^{-1}(U'_i) / \sim & \quad (\mathbb{G}_m^{an})^2 \\ & \supseteq \quad \subseteq \\ & \mathfrak{Trop}_i^{-1}(U_i) \end{aligned}$$

To distinguish the two inclusion, we will always view  $\mathfrak{Trop}_i^{-1}(U_i)$  as a subset of  $(\mathbb{G}_m^{an})^2$  and consider

$$\alpha_i : \mathfrak{Trop}_i^{-1}(U_i) \rightarrow \check{X}.$$

Notice that  $\mathfrak{Trop}_i^{-1}(U'_i)$  only occupies a small portion of  $(\mathbb{G}_m^{an})^2$ . Thus we need to extend  $\alpha_i$  to most part of  $(\mathbb{G}_m^{an})_i^2$ . For the simplicity of the notation, we will still denote those extension of  $\alpha_i$  be the same notation.

Now we want to understand how  $\mathcal{U}'_i$  glue with  $\mathcal{U}'_{i+1}$ . Let  $V_i, V_{i+1}$  be any small enough rational domains on  $B_0$  such that  $V_i \subseteq U'_i$ ,  $V_{i+1} \subseteq U'_{i+1}$  and the Fukaya's trick applies. Let  $p \in V_i \cap V_{i+1}$  be the reference point and one has

$$(\mathbb{G}_m^{an})_i^2 \supseteq \mathfrak{Trop}_i^{-1}(V_i) \supseteq \mathfrak{Trop}_i^{-1}(V_i \cap V_{i+1}) \xrightarrow{\Psi_{i,i+1}} \mathfrak{Trop}_{i+1}^{-1}(V_i \cap V_{i+1}) \subseteq \mathfrak{Trop}_{i+1}^{-1}(V_{i+1}) \subseteq (\mathbb{G}_m^{an})_{i+1}^2,$$

where  $\Phi_{i,i+1} = \alpha_{i+1}^{-1} \circ \alpha_i$  is given by  $\Psi_{i,i+1} = S_{u_{i+1},p}^{-1} \circ \Phi_{i,i+1} \circ S_{u_i,p}$  by (16) and

$$\Phi_{i,i+1} : z^{\partial\gamma} \mapsto z^{\partial\gamma} (1 + T^{\omega(\gamma_{i+1})} z^{\partial\gamma_i})^{\langle \gamma, \gamma_{i+1} \rangle}$$

from Definition 4.3 and Theorem 5.8. Here  $\omega(\gamma_{i+1})$  is evaluated at  $p$ . From (26), we have  $\langle \gamma_{i+1}, \gamma_i \rangle = 1$ . Then with the notation and discussion below Remark 5.12, we have  $\Phi_{i,i+1}$  is simply the polynomial map

$$\begin{aligned} z^{\gamma_i} &\mapsto z^{\gamma_i} (1 + z^{\gamma_{i+1}})^{-1} \\ z^{\gamma_{i+1}} &\mapsto z^{\gamma_{i+1}}. \end{aligned} \tag{29}$$

Since near  $l_{\gamma_{i+1}}$  one has  $\omega(\gamma_{i+1}) > 0$ , one has

$$\text{val}(z^\gamma) = \text{val}(z^\gamma (1 + z^{\gamma_i})^{-1}). \tag{30}$$

Here we view  $z^\gamma$  as a function on  $(\Lambda^*)^2$  and  $\text{val}$  is the valuation on  $\Lambda^*$ . Thus, the following commutative diagram holds under the identification  $(\Lambda^*)^2 \cong (\mathbb{G}_m^{an})^2$ ,

$$\begin{array}{ccc} \mathfrak{Trop}_i^{-1}(V_i) \supseteq \mathfrak{Trop}_i^{-1}(V_i \cap V_{i+1}) & \xrightarrow{\Phi_{i,i+1}} & \mathfrak{Trop}_{i+1}^{-1}(V_i \cap V_{i+1}) \subseteq \mathfrak{Trop}_{i+1}^{-1}(V_{i+1}) \\ \downarrow \mathfrak{Trop}_i & & \downarrow \mathfrak{Trop}_{i+1} \\ \mathbb{R}_i^2 \supseteq V_i \cap V_{i+1} & \xlongequal{\quad} & V_i \cap V_{i+1} \subseteq \mathbb{R}_{i+1}^2 \end{array} \tag{31}$$

We may view  $(\Lambda^*)^2$  as the  $\Lambda$ -points of the scheme  $(\mathbb{G}_m)^2 = \text{Spec} \Lambda[z^{\pm\gamma_i}, z^{\pm\gamma_{i+1}}]$ . Then we have the commutative diagram from GAGA functor

$$\begin{array}{ccc} (\mathbb{G}_m^{an})^2 & \xrightarrow{\Psi_{i,i+1}} & (\mathbb{G}_m^{an})^2 \\ \text{GAGA} \uparrow & & \uparrow \text{GAGA} \\ (\mathbb{G}_m)^2 & \longrightarrow & (\mathbb{G}_m)^2 \end{array} \tag{32}$$

Under the identification  $(\Lambda^*)^2 \cong (\mathbb{G}_m^{an})^2$ ,  $\Psi_{i,i+1}$  is simply the restriction of the map  $(\mathbb{G}_m^{an})^2 \rightarrow (\mathbb{G}_m^{an})^2$  with the same equation as in (29). Therefore, we have the same commutative diagram as in (31) with  $V_i, V_{i+1}$  replaced by  $U_i^+, U_{i+1}$  for any open subset  $U_i^+ \subseteq \mathbb{R}^2$  such that  $\omega(\gamma_{i+1}) > 0$  on  $U_i^+$ , which we will choose it explicitly later.

To see the largest possible extension  $U_i^+$  and thus largest possible extension of the above diagram, we would want to know explicitly where  $\omega(\gamma_{i+1}) > 0$ . Viewing  $B \cong \mathbb{C}$ , we may take  $U_i^+$  as the interior of the sector bounded by  $l_{\gamma_i}$  and the ray by rotating  $\frac{3\pi}{5}$  counter-clockwisely from  $l_{\gamma_{i+1}}$  by Lemma 5.6 and this is the largest possible region (extending  $U_i$  counter-clockwisely) such that  $\omega(\gamma_{i+1}) > 0$  holds. In particular,  $U_i^+$  occupies  $U_i, U_{i+1}$  and half of  $U_{i+2}$ . Therefore, we have the following lemma

**Lemma 5.13.** *The inclusion  $\alpha_i : \mathfrak{Trop}_i^{-1}(U_i) \hookrightarrow \check{X}$  can be extended to  $\alpha_i : \mathfrak{Trop}_i^{-1}(U_i^+) \hookrightarrow \check{X}$ ,  $i = 1, \dots, 5$ . In particular,  $\alpha_i(\mathfrak{Trop}_i(U_i \cup U_{i+1})) \subseteq \check{X}$ . Here we use the convention  $U_{i+5} = U_i$ .*

To further extend  $\alpha_i$ , the commutative diagram (31) no longer holds since

$$\text{val}(z^{\gamma_i}(1 + z^{\gamma_{i+1}})^{-1}) = \text{val}(z^{\gamma_i}) - \text{val}(1 + z^{\gamma_{i+1}}) = \text{val}(z^{\gamma_i}) - \text{val}(z^{\gamma_{i+1}}) \quad (33)$$

outside of  $U_i^+$ , which is no longer  $\text{val}(z^{\gamma_i})$  on the right hand side as in (30). Now for  $V_i$  disjoint from  $U_i^+$  and  $V_{i+1} \subseteq U_{i+2} \subseteq U_{i+1}^+$ , the diagram becomes

$$\begin{array}{ccc} \mathfrak{Trop}_i^{-1}(V_i) \supseteq \mathfrak{Trop}_i^{-1}(V_i \cap V_{i+1}) \setminus \{1 + z^{\gamma_{i+1}} = 0\} & \xrightarrow{\Psi_{i,i+1}} & \mathfrak{Trop}_i^{-1}(V_i \cap V_{i+1}) \subseteq (\mathbb{G}_m^{an})^2 \\ \downarrow \mathfrak{Trop}_i & & \downarrow \mathfrak{Trop}_{i+1} \\ \mathbb{R}_i^2 \supseteq V_i \cap V_{i+1} & \xrightarrow{\phi_{i,i+1}} & \mathbb{R}_{i+1}^2 \end{array} \quad (34)$$

Recall that

$$\text{val}(z^{\gamma_i}) = \int_{\gamma_i} \omega = x_i, \quad \text{val}(z^{\gamma_{i+1}}) = \int_{\gamma_{i+1}} \omega = y_i$$

from (19) and thus together with (33) we have

$$\begin{aligned} \phi_{i,i+1} : x_i &\mapsto x_i - y_i \\ y_i &\mapsto y_i \end{aligned} \quad (35)$$

on its domain. Notice that  $\Psi_{i,i+1}$  is only defined when  $1 + z^{\gamma_{i+1}} \neq 0$ . Since the linear map (35) is well-defined on  $\mathbb{R}^2$ , we will still use the same notation for such natural extension.

**Lemma 5.14.**  $\phi_{i,i+1}(U_{i+2} \setminus U_i^+) \subseteq U_{i+1}^+$ . In particular,

$$\alpha_i(\mathfrak{Trop}_i^{-1}(U_{i+2})) \subseteq \alpha_{i+1}(\mathfrak{Trop}_{i+1}^{-1}(U_{i+1}^+)) \subseteq \check{X}.$$

*Proof.* The left boundary of  $U_i^+$  is characterized by  $x_{i+1} = 0, y_{i+1} > 0$  and the left boundary of  $U_{i+1}^+$  is characterized by  $x_{i+1} < 0, y_{i+1} = 0$  from Lemma 5.6. Therefore, we may identify the region bounded by the above two affine lines with the third quadrant of  $\mathbb{R}_{x_{i+1}, y_{i+1}}^2$  as affine manifolds. Notice that this is a subset of  $U_{i+1}^+$ . Under such identification, we have  $U_{i+2} \setminus U_i^+$  as the region bounded by  $x_{i+1} + y_{i+1} = 0$  and  $y_{i+1}$ -axis in the third quadrant by Lemma 5.11. In terms of  $(x_{i+1}, y_{i+1})$ , (35) becomes

$$\begin{aligned} \phi_{i,i+1} : x_{i+1} &\mapsto x_{i+1} \\ y_{i+1} &\mapsto x_{i+1} + y_{i+1}, \end{aligned}$$

from the relation  $\gamma_i + \gamma_{i+2} = \gamma_{i+1}$ . The lemma then follows from direct computation.  $\square$

To sum up, one can extend the original inclusion  $\alpha_i(\mathfrak{Trop}_i^{-1}(U_i)) \subseteq \check{X}$  in the counter-clockwise direction to

$$\alpha_i(\mathfrak{Trop}_i^{-1}(\overline{U_i \cup U_{i+1} \cup U_{i+2}}) \setminus \{1 + z^{\gamma_{i+1}} = 0\}) \subseteq \check{X}. \quad (36)$$

Here we use  $\overline{U}$  to denote the interior of the compactification of  $U$ .

**Lemma 5.15.** *The inclusion (36) extends over  $\{1 + z^{\gamma_{i+1}} = 0\} \setminus \mathfrak{Trop}_i^{-1}(0)$ .*

*Proof.* Let  $W_i$  be small neighborhood of (a component of)  $\partial U_i^+$  such that  $\{1 + z^{\gamma_{i+1}} = 0\} \subseteq \mathfrak{Trop}_i^{-1}(W_i)$ . Notice that from Lemma 5.14, we have that  $\mathfrak{Trop}(\alpha_i(\mathfrak{Trop}_i^{-1}(W_i))) \subseteq U_{i+2}$ . We will show that

$$\alpha_i(\mathfrak{Trop}_i^{-1}(W_i)) \subseteq \alpha_{i+1}(\mathfrak{Trop}_{i+1}^{-1}(U_{i+1}^+)) \cup \alpha_{i+2}(\mathfrak{Trop}_{i+2}^{-1}(U_{i+2})) \cup \alpha_{i+3}(\mathfrak{Trop}_{i+3}^{-1}(U_{i+2})). \quad (37)$$

From the earlier discussion, we have

$$\alpha_i(\mathfrak{Trop}_i^{-1}(W_i) \setminus \{1 + z^{\gamma_{i+1}} = 0\}) \subseteq \alpha_{i+1}(\mathfrak{Trop}_{i+1}^{-1}(U_{i+1}^+)).$$

From the earlier discussion, we have

$$\begin{aligned} \Psi_{i+1,i+2} : \mathfrak{Trop}_{i+1}^{-1}(U_{i+2}) &\cong \mathfrak{Trop}_{i+2}^{-1}(U_{i+2}) \\ \Psi_{i+3,i+2} : \mathfrak{Trop}_{i+3}^{-1}(U_{i+2}) &\cong \mathfrak{Trop}_{i+2}^{-1}(U_{i+2}). \end{aligned} \quad (38)$$

Recall that  $\Psi_{i,j} = \alpha_j^{-1} \circ \alpha_i$ . It suffices to check that

$$A = \{1 + z^{\gamma_{i+1}} = 0\} \subseteq \Psi_{i+2,i}(\mathfrak{Trop}_{i+2}^{-1}(U_{i+2})) \cup \Psi_{i+3,i}(\mathfrak{Trop}_{i+3}^{-1}(U_{i+2})) \quad (39)$$

as subsets of  $(\mathbb{G}_m^{an})_i^2$ . Straight calculation shows that

$$\begin{aligned} \Psi_{i,i+2} : \mathfrak{Trop}_i^{-1}(W_i) &\rightarrow \mathfrak{Trop}_{i+2}(U_{i+2}) \\ z^\gamma &\mapsto z^\gamma (1 + z^{\gamma_{i+2}})^{\langle \gamma, \gamma_{i+2} \rangle} \left( 1 + \frac{z^{\gamma_{i+1}}}{1 + z^{\gamma_{i+2}}} \right)^{\langle \gamma, \gamma_{i+1} \rangle} \end{aligned}$$

Since  $\langle \gamma, \gamma_{i+2} \rangle > 0$  and  $\langle \gamma, \gamma_{i+1} \rangle > 0$  over  $U_{i+2}$ . We have  $\Psi_{i,i+2}$  is not defined only on

$$B = \{1 + z^{\gamma_{i+2}} = 0\} \cup \{1 + z^{\gamma_{i+1}} + z^{\gamma_{i+2}} = 0\}.$$

Therefore, we have  $\alpha_i$  can be extended over  $\mathfrak{Trop}_i^{-1}(W_i) \setminus B$ . Similarly,  $\Psi_{i,i+3}$  is defined except

$$C = \{1 + z^{\gamma_{i+3}} = 0\} \cup \{1 + z^{\gamma_{i+2}} + z^{\gamma_{i+3}} = 0\} \cup \{1 + z^{\gamma_{i+1}} + z^{\gamma_{i+2}} + z^{\gamma_{i+3}} = 0\}.$$

Therefore,  $\alpha_i$  can be extended over  $\mathfrak{Trop}_i^{-1}(W_i) \setminus C$ . It is easy to check that  $A \cap B \cap C = \{z^{\gamma_{i+1}} = z^{\gamma_{i+2}} = -1\} \subseteq \mathfrak{Trop}^{-1}(0)$ . Since  $\Psi_{i,j} = \alpha_j^{-1} \circ \alpha_i$  and thus the extension is compatible. Now the lemma is proved.  $\square$

For the same reason, one can extend the inclusion in the clockwise direction

$$\alpha_i(\mathfrak{Trop}_i^{-1}(\overline{U_i \cup U_{i-1} \cup U_{i-2}})) \subseteq \check{X}. \quad (40)$$

Notice that  $l_{\gamma_{i+3}} = l_{\gamma_{i-2}}$  is the the boundary of both  $U_{i+2}$  and  $U_{i-2}$ . Then (36)(40) together imply the inclusion

$$\alpha_i(\mathfrak{Trop}_i^{-1}(\mathbb{R}^2 \setminus l_{\gamma_{i+3}})) \subseteq \check{X}. \quad (41)$$

Then Lemma 5.16 below guarantees that the inclusion extends over the ray  $l_{\gamma_k}$  and we reach an extension

$$\alpha_i : \mathfrak{Trop}_i^{-1}(\mathbb{R}^2 \setminus \{0\}) \rightarrow \check{X}.$$

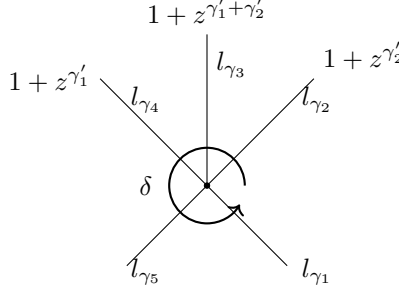
Finally we claim that  $\alpha_i$  is an embedding restricting on  $\mathfrak{Trop}^{-1}(U)$  for small enough open subset  $U \subseteq \mathbb{R}^2$ . On the other hand,  $\alpha_i$  is fibre-preserving with respect to  $\mathfrak{Trop}_i : (\mathbb{G}_m^{an})^2 \rightarrow \mathbb{R}^2$  and  $\mathfrak{Trop} : \check{X} \rightarrow B$  and the induced map on the base is piecewise-linear. Direct computation shows that induced map on the base is injective. Therefore,  $\alpha_i$  is an embedding. Therefore  $\check{X}$  has a partial compactification  $\bigcup_{i=1}^5 (\mathbb{G}_m^{an})_i^2 / \sim$ , with the identification  $\Psi_{i,j} : (\mathbb{G}_m^{an})_i^2 \rightarrow (\mathbb{G}_m^{an})_j^2$ .

**Lemma 5.16.** *The composition of the wall-crossing transformations cancel out the monodromy. Explicitly,*

$$\mathcal{K}_{\gamma_5} \mathcal{K}_{\gamma_4} \mathcal{K}_{\gamma_3} \mathcal{K}_{\gamma_2} \mathcal{K}_{\gamma_1}(z^{\partial \gamma}) = z^{M^{-1}(\partial \gamma)}.$$

*Proof.* We will use the identification as in (29). Let us consider  $a = a_1\gamma'_1 + a_2\gamma'_2 \in H_1(L_p, \mathbb{Z})$ , where  $p \in B_0$  is a reference point, and a loop from  $l_{\gamma_1}$  anticlockwise to itself:

We will first compute the case without any singularities. This is very standard from [23]. We are only repeating it as there may be confusion about signs.



**Remark 5.17.** Before we go into the calculation, let us unfold the sign convention in Theorem 4.2. To determine the sign, we have the condition  $\text{Arg}Z_\gamma(u_-) < \text{Arg}Z_\gamma(u_+)$ . This means that the loop  $\delta$  is going in anti-clockwise direction.

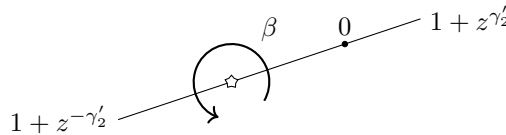
In the calculation of the exponents, we consider  $\gamma \mapsto \langle \cdot, \gamma \rangle$ . Note that  $\langle \cdot, \cdot \rangle$  is the intersection pairing but not the usual inner product. Together with  $\langle \gamma'_1, \gamma'_2 \rangle = 1$ , we have  $\langle \cdot, \gamma \rangle$  is the normal of  $l_\gamma$  pointing in the same direction as  $\delta$  in the language of [23].

Let us consider the transformation  $\mathcal{K}_\delta = \mathcal{K}_{\delta, l_{\gamma_1}} \mathcal{K}_{\delta, l_{\gamma_5}} \mathcal{K}_{\delta, l_{\gamma_4}} \mathcal{K}_{\delta, l_{\gamma_3}} \mathcal{K}_{\delta, l_{\gamma_2}}$ , where  $\mathcal{K}_{\delta, l_{\gamma_k}} = \mathcal{K}_{\gamma_k}$  for  $k = 1, 2, 3$ ;  $\mathcal{K}_{\delta, l_{\gamma_{k+3}}} = \mathcal{K}_{\gamma_k}$  for  $k = 1, 2$ .

To simplify the notation, we will denote  $\xrightarrow{\mathcal{K}_{\delta, l_{\gamma_k}}}$  for the wall crossing over the wall  $l_{\gamma_k}$  according to the curve  $\delta$ .

$$\begin{aligned}
z^a &\xrightarrow{\mathcal{K}_{\delta, l_{\gamma_2}}} z^a (1 + z^{\gamma'_2})^{a_1}, \\
&\xrightarrow{\mathcal{K}_{\delta, l_{\gamma_3}}} z^a (1 + z^{\gamma'_1 + \gamma'_2})^{a_1 - a_2} \left(1 + z^{\gamma'_2} (1 + z^{\gamma'_1 + \gamma'_2})^{-1}\right)^{a_1}, \\
&= z^a (1 + z^{\gamma'_1 + \gamma'_2})^{-a_2} (1 + z^{\gamma'_2} + z^{\gamma'_1 + \gamma'_2})^{a_1}, \\
&\xrightarrow{\mathcal{K}_{\delta, l_{\gamma_4}}} z^a (1 + z^{\gamma'_1})^{-a_2} \left(1 + z^{\gamma'_1 + \gamma'_2} (1 + z^{\gamma'_1})^{-1}\right)^{-a_2} \left(1 + z^{\gamma'_2} (1 + z^{\gamma'_1})^{-1} (1 + z^{\gamma'_1})\right)^{a_1}, \\
&= z^a (1 + z^{\gamma'_1} + z^{\gamma'_1 + \gamma'_2})^{-a_2} (1 + z^{\gamma'_2})^{a_1}, \\
&\xrightarrow{\mathcal{K}_{\delta, l_{\gamma_5}}} z^a (1 + z^{\gamma'_2})^{-a_1} \left(1 + z^{\gamma'_1} (1 + z^{\gamma'_2})^{-1} (1 + z^{\gamma'_2})\right)^{-a_2} (1 + z^{\gamma'_2})^{a_1} \\
&= z^a (1 + z^{\gamma'_1})^{-a_2}, \\
&\xrightarrow{\mathcal{K}_{\delta, l_{\gamma_1}}} z^a (1 + z^{\gamma'_1})^{a_2} (1 + z^{\gamma'_1})^{-a_2}, \\
&= z^a.
\end{aligned}$$

Thus we obtain the consistency as usual. Next we investigate the wall crossing transformation over the monodromy deduced by focus-focus singularities on  $l_{\gamma'_2}$ .



Let us consider the wall crossing  $\mathcal{K}_\beta = \mathcal{K}_{\beta, 2} \mathcal{K}_{\beta, 1}$  over the curve  $\beta$ , where  $\mathcal{K}_{\beta, 1} = \mathcal{K}_{\gamma'_2}$ , and  $\mathcal{K}_{\beta, 2} = \mathcal{K}_{-\gamma'_2}$ .

The first wall crossing will lead us to

$$\mathcal{K}_{\beta,1}(z^a) = z^a(1 + z^{\gamma'_2})^{a_1}.$$

Then passing over the wall again by using  $\beta$  will get us

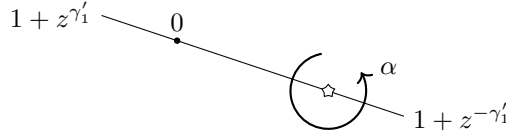
$$\begin{aligned}\mathcal{K}_{\beta}(z^a) &= \mathcal{K}_{\beta,2} \circ \mathcal{K}_{\beta,1}(z^a) = z^a(1 + z^{-\gamma'_2})^{-a_1}(1 + z^{\gamma'_2})^{a_1} \\ &= z^{a_1\gamma'_1 + (a_1 + a_2)\gamma'_2}.\end{aligned}$$

To have  $z^{a_1\gamma'_1 + (a_1 + a_2)\gamma'_2}$  goes back to  $z^a$ , we have the monodromy  $M_2$

$$\gamma'_1 \mapsto \gamma'_1 - \gamma'_2, \quad (42)$$

$$\gamma'_2 \mapsto \gamma'_2. \quad (43)$$

Let us first consider the monodromy over the focus-focus singularities on  $l_{\gamma'_1}$ :



Consider the transformation according to the loop  $\alpha$ . Let  $\mathcal{K}_{\alpha,1} = \mathcal{K}_{\gamma'_1}$ , and  $\mathcal{K}_{\alpha,2} = \mathcal{K}_{-\gamma'_1}$ . We have

$$\mathcal{K}_{\alpha,1}(z^a) = z^a(1 + z^{\gamma'_1})^{-a_2}.$$

Then the whole loop  $\alpha$  leads us to

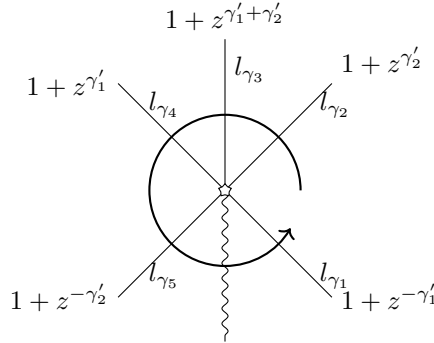
$$\begin{aligned}\mathcal{K}_{\alpha} &= \mathcal{K}_{\alpha,2} \circ \mathcal{K}_{\alpha,1}(z^a) = z^a(1 + z^{-\gamma'_1})^{a_2}(1 + z^{\gamma'_1})^{-a_2} \\ &= z^{(a_1 - a_2)\gamma'_1 + a_2\gamma'_2}.\end{aligned}$$

Then we obtain the monodromy  $M_1$

$$\gamma'_1 \mapsto \gamma'_1, \quad (44)$$

$$\gamma'_2 \mapsto \gamma'_1 + \gamma'_2. \quad (45)$$

Thus, we can compute the monodromy while singularity is at the origin. There are two ways checking it. The first one is doing a similar calculation as in the beginning of the proof. Now we consider



The first three wall crossings are the same and let us recap here:

$$\mathcal{K}_{\delta, l_{\gamma_4}} \mathcal{K}_{\delta, l_{\gamma_3}} \mathcal{K}_{\delta, l_{\gamma_2}}(z^a) = z^a(1 + z^{\gamma'_1} + z^{\gamma'_1 + \gamma'_2})^{-a_2}(1 + z^{\gamma'_2})^{a_1}.$$



Now to pass over  $l_{\gamma_5}$ , we will have

$$\begin{aligned}\mathcal{K}(z^a(1+z^{\gamma'_1}+z^{\gamma'_1+\gamma'_2})^{-a_2}(1+z^{\gamma'_2})^{a_1}) &= z^a(1+z^{-\gamma'_2})^{-a_1}\left(1+z^{\gamma'_1}(1+z^{-\gamma'_2})^{-1}(1+z^{\gamma'_2})\right)^{-a_2}(1+z^{\gamma'_2})^{a_1} \\ &= z^{a_1\gamma'_1+(a_1+a_2)\gamma'_2}(1+z^{\gamma'_1+\gamma'_2})^{-a_2}.\end{aligned}$$

The monodromy  $M$  would then be

$$\begin{aligned}\gamma'_1 &\mapsto -\gamma'_2; \\ \gamma'_2 &\mapsto \gamma'_1 + \gamma'_2.\end{aligned}$$

and gives us

$$\mathcal{K}_M(z^{a_1\gamma'_1+(a_1+a_2)\gamma'_2}(1+z^{\gamma'_1+\gamma'_2})^{-a_2}) = z^{(a_1+a_2)\gamma'_1+a_2\gamma'_2}(1+z^{\gamma'_1})^{-a_2}.$$

The last wall crossing would then be

$$\begin{aligned}\mathcal{K}_{\delta, l_{\gamma_1}}\left((z^{(a_1+a_2)\gamma'_1+a_2\gamma'_2}(1+z^{\gamma'_1})^{a_1})\right) &= z^{(a_1+a_2)\gamma'_1+a_2\gamma'_2}(1+z^{-\gamma'_1})^{a_2}(1+z^{\gamma'_1})^{-a_2} \\ &= z^a.\end{aligned}$$

The second way is to use the following meta-lemma by direct computation

**Claim 5.18.**  $\mathcal{K}_{-\gamma}\mathcal{K}_\gamma(z^{\gamma'}) = z^{M^{-1}\gamma'}$ , where  $M$  is transformation  $\gamma' \mapsto \gamma' + \langle \gamma, \gamma' \rangle \gamma$ .

Note that if  $\gamma$  is primitive, then  $M$  is the Picard-Lefschetz transformation of a focus-focus singularity with Lefschetz thimble  $\gamma$ . Recall that if  $\langle \gamma', \gamma \rangle = 1$ , then the pentagon equation reads

$$\mathcal{K}_\gamma\mathcal{K}_{\gamma'} = \mathcal{K}_{\gamma'}\mathcal{K}_{\gamma+\gamma'}\mathcal{K}_\gamma. \quad (46)$$

Let  $M_1, M_2$  denote the transformation in the Claim 5.18 with respect to  $\gamma'_1, \gamma'_2$  respectively.

With the branch cut as in Figure 3, one has

$$\mathcal{K}_{\gamma_5}\mathcal{K}_{\gamma_4}\mathcal{K}_{\gamma_3}\mathcal{K}_{\gamma_2}\mathcal{K}_{\gamma_1} = \left(\mathcal{K}_{-\gamma_2}\mathcal{K}_{\gamma_2}\right)\left(\mathcal{K}_{\gamma_2}^{-1}\mathcal{K}_{\gamma_4}\mathcal{K}_{\gamma_3}\mathcal{K}_{\gamma_2}\mathcal{K}_{-\gamma_1}^{-1}\right)\left(\mathcal{K}_{-\gamma_1}\mathcal{K}_{\gamma_1}\right).$$

Notice that the middle of the right hand side is identity by the pentagon identity (46). From Lemma 5.18, we have

$$\mathcal{K}_{\gamma_5}\mathcal{K}_{\gamma_4}\mathcal{K}_{\gamma_3}\mathcal{K}_{\gamma_2}\mathcal{K}_{\gamma_1}(z^\gamma) = z^{M_2^{-1}M_1^{-1}\gamma} = z^{(M_1M_2)^{-1}\gamma}$$

and the lemma follows from the fact that  $M = M_1M_2$ . Notice the the proof is motivated by deforming the type  $II$  singular fibre into two  $I_1$  singular fibres as in Figure 5. However, the proof does NOT depend on the actual geometric deformation.

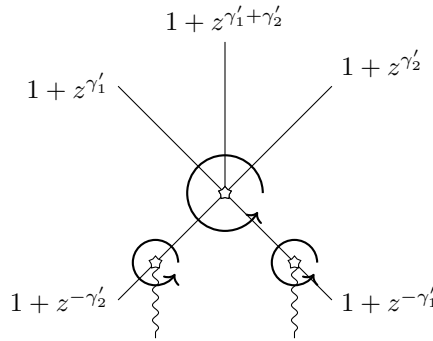


Figure 5: Geometric interpretation of Lemma 5.16.

□

**Remark 5.19.** *It worth noticing that the above calculation a priori may be different from the composition of wall-crossing for the  $A_2$  cluster variety for two reasons. The first difference comes from the appearance of the monodromy at the origin while there is no such in the cluster scattering diagram. We will explain the identification in Section 5.3. The second difference comes from the fact that the in the calculation for cluster variety there is a preferred choice of basis in each chamber while the calculation in Floer theory uses a fixed basis (up to parallel transport). However, thanks to (26), the two calculations thus coincide.*

In next section, we will show that the later has a compactification to the analytification of the del Pezzo surface of degree five by adding a cycle of five rational curves via ring of theta functions following [24].

**Remark 5.20.** *One would naturally expect that the family Floer mirror of the hyperKähler rotation of  $X'_t$  still compactifies to the del Pezzo surface of degree five. In this case, one there is only two families of holomorphic discs in each of the singularities and one can glue the local model in [32, Section 8] and get a partial compactification of the family Floer mirror. The author will compare it with the Gross-Siebert construction of the mirror in the future work.*

**Remark 5.21.** *Shen-Zaslow-Zhou uses the homological mirror symmetry for the  $A_2$  cluster variety with an canonical equivariant  $\mathbb{Z}_5$  action [42]*

## 5.2 Comparison with GHK Mirror of $dP_5$

Let  $Y$  be the del Pezzo surface of degree five and  $D$  be the anti-conical divisor consists of wheel of five rational curves. Here we will explain the comparison of the family Floer mirror of  $X_{II}$  with the GHK mirror of  $(Y, D)$ . Recall that in Lemma 5.9, we identify the integral affine structures on  $B_0$  and  $B_{\text{GHK}}$ . Moreover, the BPS rays naturally divide  $B_0$  into cones which is exactly the cone decomposition of  $B_{\text{GHK}}$ . The canonical scattering diagram in this case is computed in [24, Example 3.7] and all the  $\mathbb{A}^1$ -curves are shown in Figure 8.

**Lemma 5.22.** *There exists a homeomorphism  $X_{II} \cong Y \setminus D$ .*

*Proof.* From the explicit equation in Section 3, a deformation of  $X_{II}$  has two singular fibres of type  $I_1$  and the vanishing cycles has intersection number 1. On the other hand, [4, Example 3.1.2] provides the local model of Lagrangian fibration near the blow-up of a point on the surface. Since  $Y$  can be realized as the blow up of two non-toric boundary point on del Pezzo surface of degree 7, One can topologically glue the pull-back of the moment map torus fibration with the local Lagrangian fibration to get a torus fibration on  $Y \setminus D$  with two nodal fibres such that the vanishing cycles has intersection 1. This gives the homeomorphism between  $X_{II}$  and  $Y \setminus D$  topologically and the identification of the class of tori among  $H_2(X_{II}, \mathbb{Z}) \cong H_2(Y \setminus D, \mathbb{Z})$ . In particular, we can use  $Y$  as an auxiliary topological compactification of  $X_{II}$ .  $\square$

We will take  $P = \text{NE}(Y)$  in the Gross-Hacking-Keel construction. We have  $P_{\mathbb{R}}^{gp} \cong \text{Pic}(Y)^* \cong H_2(Y, \mathbb{Z})$ , where the first isomorphism comes from Poincare duality and  $Y$  is projective while the second isomorphism comes from  $H^{1,0}(Y) = H^{2,0}(Y) = 0$ . The rank two lattice  $H_1(L_u, \mathbb{Z})$  glues to a local system of lattice over  $B_0$  and is naturally identified with  $\Lambda_{B_0}$  by Remark 3.2. Then we have the commutative diagram except the middle map. Here  $\underline{H_2(Y, \mathbb{Z})}$  denotes the constant sheaf with fibre  $H_2(Y, \mathbb{Z})$  over  $B_0$ .

$$\begin{array}{ccccccc}
0 & \longrightarrow & \underline{H_2(Y, \mathbb{Z})} & \longrightarrow & \bigcup_{u \in B_0} H_2(Y, L_u) & \xrightarrow{\partial} & \bigcup_{u \in B_0} H_1(L_u, \mathbb{Z}) \longrightarrow 0 \\
& & \downarrow \cong & & \downarrow \Psi & & \downarrow \cong \\
0 & \longrightarrow & P_{\mathbb{R}}^{gp} & \longrightarrow & \mathcal{P} & \xrightarrow{r} & \Lambda_{B_0} \longrightarrow 0
\end{array} \tag{47}$$

Next we will construct the middle map  $\Psi$ . Recall that a neighborhood of  $D$  is covered by charts  $W_i = \{(x_i, y_i) \in \mathbb{C}^2 \mid |x_i y_i| < 1\}$  such that

1.  $(Y, D)$  is modeled by  $(W_i, \{x_i y_i = 0\})$  near a node  $D_i \cap D_{i+1}$
2.  $D_i = \{x_i = 0\}$  and  $D_{i+1} = \{y_i = 0\}$

$$3. \ x_{i+1} = y_i^{-1}, y_{i+1} = x_i y_i^{-D_i^2}.$$

Notice that  $N_{D_i/Y} \cong \mathcal{O}_{\mathbb{P}^1}(D_i^2)$  and the last equation comes from the transition functions for  $\mathcal{O}_{\mathbb{P}^1}(D_i^2)$ . The torus fibre in  $Y \setminus D$  near the node  $D_i \cap D_{i+1}$  is isotopic to  $L = \{|x_i| = |y_i| = \frac{1}{2}\}$ . It is easy to see that  $L$  bounds two families of holomorphic discs  $\{|x_i| \leq \frac{1}{2}, y_i = \text{const}\}$  and  $\{x_i = \text{const}, |y_i| \leq \frac{1}{2}\}$ . Denote  $\beta_i \in H_2(Y, \mathbb{Z})$  be relative class of the discs intersecting  $D_i$  and represented by the 2-chain  $b_i$ . Over the simply connected subset  $U_i \subseteq B_0$ , both of the short exact sequence in (47) splits (non-canonically) and we define the middle map by  $\Psi(\phi_{\rho_i}(v_i)) = \beta_i$ . From Remark 3.2, the right hand side square commutes and  $\partial\beta_i$  (up to parallel transport) generate  $H_1(L_u, \mathbb{Z})$ . Therefore, the five lemma implies  $\Psi$  is an isomorphism over  $U_i$  and the two short exact sequences in (47) over  $U_i$  are identified. To see that the middle map is independent of  $i$ , one has the following observation: We may choose  $u$  to be in a neighborhood of  $D_i$ , which is diffeomorphic to  $N_{D_i/Y} \cong \mathcal{O}_{\mathbb{P}^1}(D_i^2)$ .

The relation  $x_{i+1} = y_i^{-1}, y_{i+1} = x_i y_i^{-D_i^2}$  translates to  $\partial\beta_{i-1} + D_i^2 \partial\beta_i + \partial\beta_{i+1} = 0 \in H_1(L, \mathbb{Z})$ , which is the analogue of (1). Therefore, there exists a 2-chain  $C$  in  $L$  such that  $C \cup b_{i-1} \cup D_i^2 b_i \cup b_{i+1}$  is a 2-cycle in the neighborhood of  $D_i$ . To see lifting the relation (1) in  $\bigcup_{u \in B_0} H_2(Y, L_u)$ , notice that the 2-cycle falls  $Y \setminus \bigcup_{j \neq i-1, i, i+1} D_j$ , which is homeomorphic to the total space of  $\mathcal{O}_{\mathbb{P}^1}(D_i^2)$ , which has its second homology generated by  $[D_i]$ . Therefore, the 2-cycle must be a multiple of  $[D_i]$ . On the other hand, the intersection number of the 2-cycle with  $D_{i-1}, D_{i+1}$  are both 1 from the explicit representative chosen and thus

$$\beta_{i-1} + D_i^2 \beta_i + \beta_{i+1} = [D_i], \quad (48)$$

which is the analogue of (4).

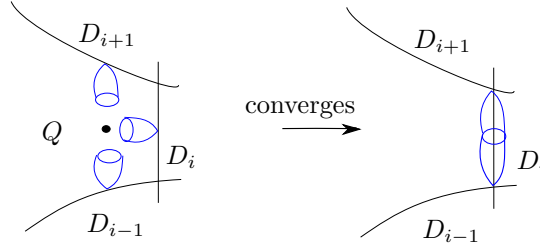


Figure 6: Illustration for (48).

Therefore, the middle map is well-defined from (48) and the middle map is an isomorphism by the five lemma. Notice that  $\beta_i + \gamma_i$  represents a 2-chain, which defines a 2-cycle up to a multiple of the fibre. Since the fibre is contractible in  $Y$ , thus we may view  $\beta_i + \gamma_i$  as a 2-cycle in  $H_2(Y, \mathbb{Z})$ . Notice that  $[E_i]$  is the unique class with intersections  $[E_i] \cdot [D_j] = \delta_{ij}$ , we have  $z^{[E_i] - \phi_{\rho_i}(v_i)}$  identified with  $z^{\gamma_i}$  (see Figure 7).

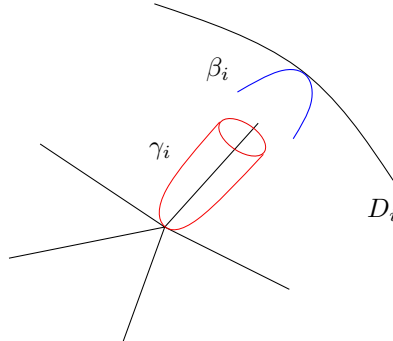


Figure 7: The class  $[E_i]$  decomposes into sum of  $\gamma_i$  and  $\beta_i$

In particular, the transformation  $\Psi_{i,i+1}$  coincides with (5). This will leads to the identification of  $\check{X}$  and the GHK mirror of  $(Y, D)$  as gluing to tori. Notice that the Gross-Hacking-Keel mirror of  $(Y, D)$  comes with a family over  $\text{Spec} \mathbb{C}[\text{NE}(Y)]$ . We will have to determine which particular point in  $\text{Spec} \mathbb{C}[\text{NE}(Y)]$  the

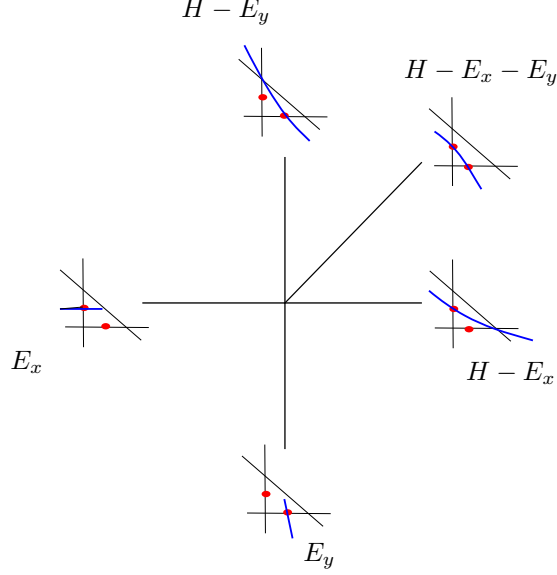


Figure 8: The canonical scattering diagram and the  $\mathbb{A}^1$ -curves in del Pezzo surfaces of degree 5 (illustrated by a projection to  $\mathbb{P}^2$ ).

family Floer mirror  $\check{X}$  corresponds to. Notice that the monodromy sends  $\gamma_i$  to  $\gamma_{i+1}$ . This implies that  $\check{X}$  corresponds to the point such that the value of  $z^{[E_i]}$  all coincides. From the explicit relation of curve classes  $[E_i]$ ,  $\check{X}$  corresponds to the point where  $z^{[D_i]} = z^{[E_i]} = 1$ .

Indeed, one can see this via the identification  $\check{X}$  with in the subset of the analytification of del Pezzo surface of degree 5. We will see in the next section (Section 5.3) that this is the cluster variety of type  $A_2$ . Recall that the Gross-Hacking-Keel mirror is determined by the algebraic equations (49) from the theta functions [24, Equation (3.2)],

$$\vartheta_{i-1}\vartheta_{i+1} = z^{[D_i]}(\vartheta_i + z^{[E_i]}).$$

Comparing with (6) (and later (49)), we see that the family Floer mirror  $\check{X}$  corresponds to the fibre with

$$z^{[D_i]} = z^{[E_i]} = 1.$$

We will show in Section 5.1, Section 5.3 and Section 5.2 the following result:

**Theorem 5.23.** *The analytification of  $\mathcal{X}$ -cluster variety of type  $A_2$  or the Gross-Hacking-Keel mirror of  $(Y, D)$  is a partial compactification of the family Floer mirror of  $X_{II}$ .*

### 5.3 Comparison with $A_2$ -Cluster Variety

In this section, we will prove that the family Floer mirror constructed in Section 5.1 is simply the  $\mathcal{X}$ -cluster variety of type  $A_2$ . The  $\mathcal{X}$ -cluster algebra of type  $A_2$  are defined in Section 2.1 with  $d_1 = d_2 = 1$ . The following observation helps to link the scattering diagram in Theorem 5.8 and  $\mathcal{X}$  the scattering diagram of type  $A_2$ .

The operation we are going to have can be viewed as a symplectic analogue of “pushing singularities to infinity” in [24]. Recall that if one has a special Lagrangian fibration with a focus-focus singularity at  $u_0$  and Lefschetz thimble  $\gamma$ . Then there exist two affine rays  $l_{\pm\gamma}$  emanating from  $u_0$  on the base, parametrizing special Lagrangian fibres bounding holomorphic discs in classes  $\pm\gamma$ . Then  $l_{\pm\gamma}$  divide a neighborhood of  $u_0$  into two chambers  $U_{\pm}$ , where  $U_{\pm}$  is characterized by  $\int_{\pm\gamma} \text{Im}\Omega > 0$ . The corresponding wall-crossing across  $l_{\pm\gamma}$  from  $U_-$  to  $U_+$  is  $\mathcal{K}_{\pm\gamma}$  and the monodromy around  $u_0$  is given by  $M$  in Claim 5.18. We make a branch cut from  $u_0$  to infinity and the parallel transport should be changed by  $M$  when crossing the branch cut. Notice that the three transformations  $\mathcal{K}_{\pm\gamma}$  and  $M$  commute. If we choose the cut coincides with  $l_{-\gamma}$ ,

then the transformation crossing  $l_{-\gamma}$  from  $U_-$  to  $U_+$  is  $K_\gamma$ , coincides with the transformation crossing  $l_\gamma$  from  $U_-$  to  $U_+$ . Similarly, if we choose the cut coincides with  $l_\gamma$ , then the transformation crossing  $l_\gamma$  from  $U_+$  to  $U_-$  is  $K_{-\gamma}$ , coincides with the transformation crossing  $l_{-\gamma}$  from  $U_+$  to  $U_-$ .

To sum up, choosing the branch cut coinciding with  $l_{-\gamma}$  makes the transformation across  $l_{\pm\gamma}$  from  $U_-$  to  $U_+$  both equal to  $K_\gamma$ , as if the singularity  $u_0$  is moved to infinity along  $l_{-\gamma}$ . Similarly, if we choose the branch cut coincides with  $l_\gamma$ , then the transformation from  $U_-$  to  $U_+$  is  $K_{-\gamma}$  as if the singularity is moved to infinity along  $l_\gamma$ .

Now back to the scattering diagram in Theorem 5.8. We can express the underlying integral affine structure on  $B_0$  in a different way by choosing different branch cuts. First we decompose  $M = M_1 M_2$ , where  $M_1, M_2$  are the Picard-Lefschetz transformations with vanishing cycles  $\gamma'_1, \gamma'_2$ . Choose the branch cut to be  $l_{\gamma_1}$  (and  $l_{\gamma_5}$ ) with the corresponding identifications to be  $M_1$  (and  $M_2$  respectively) as in Figure 9. Then from the previous discussion in this section and the same argument in Section 5.1, the family mirror is thus gluing of five tori with the gluing coincide with those of the  $A_2$ -cluster variety  $\check{X}_C$ .

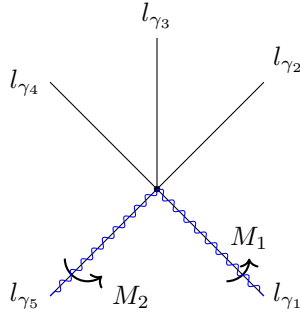


Figure 9: The different choice of branch cuts for  $X_{II}$ .

Note that one can similarly define theta function in the analytic situation. Since we are working with finite type, we can express theta functions in different torus charts by path ordered products. The functions are well defined since the scattering diagram is consistent (see Lemma 5.16). Further note that, in the finite case, we can replicate (6) to define multiplications between theta functions without broken lines<sup>12</sup>. Standard and straight-forward calculation shows that

$$\vartheta_{v_{i-1}} \cdot \vartheta_{v_{i+1}} = 1 + \vartheta_{v_i}, \quad (49)$$

where  $v_i$  denotes the primitive generator of  $l_{\gamma_i}$   $i \in \{1, \dots, 5\}$  ordered cyclically. We can see it agrees with the exchange relations as in Section 2.1. This gives a natural embedding of  $\check{X}_C$  into  $\mathbb{P}^5$  after suitable homogenization of (49) thus compactified to a del Pezzo surface of degree five.

## 6 Family Floer Mirror of $X_{III}$

In this section, we will consider the case when  $Y' = Y'_{III}$  be a rational elliptic surface with singular configuration  $III^* III$ ,  $D'$  is the type  $III^*$  fibre. We claim that the family Floer mirror of  $X = X_{III}$  is then the del Pezzo surface of degree 6. The argument is similar to that in Section 5.

First of all, such  $Y'$  has the explicit affine equation

$$y^2 = x^4 + u.$$

It is easy to see that the fibre over  $u = 0$  is a singular fibre of type  $III$ , while the fibre at infinity is of type  $III^*$ . There is a natural deformation  $Y'_t$  be the minimal resolution of the surface

$$\{z^2 y^2 = x^4 + 4t^2 x^2 z^2 + u z^4\} \subseteq \mathbb{P}^2_{(x:y:z)} \times \mathbb{P}^1_{(s:u)}$$

<sup>12</sup>In general, the products of theta functions can be expressed as the linear combination of theta functions [24, 26], which the coefficients can be computed via broken lines.

such that there are two singular fibres of type  $I_1, I_2$  with near  $u = 0$ ,  $|t| \ll 1$ . With vanishing thimbles  $\gamma'_1$  and  $\gamma'_2, \gamma'_3$ . By Theorem 4.5, we have the analogue of Theorem 5.8.

**Theorem 6.1.** [39, Theorem 4.12] *There exist  $\gamma'_1, \gamma'_2, \gamma'_3 \in H_2(X, L_u) \cong \mathbb{Z}^3$  such that  $\langle \gamma'_1, \gamma'_2 \rangle = \langle \gamma'_1, \gamma'_3 \rangle = 1$ ,  $\langle \gamma'_2, \gamma'_3 \rangle = 0$  and  $Z_{\gamma'_2} = Z_{\gamma'_3}$ . Moreover, if we set*

$$\gamma_1 = -\gamma'_1, \quad \gamma_2 = \gamma'_2, \quad \gamma_3 = \gamma'_1 + \gamma'_2 + \gamma'_3, \quad \gamma_4 = \gamma'_1 + \gamma'_2, \quad \gamma_5 = \gamma'_1, \quad \gamma_6 = -\gamma'_3.$$

Then

1.  $f_\gamma(u) \neq 1$  if and only if  $u \in l_{\gamma_i}$  and  $\gamma = \gamma_i$  for some  $i \in \{1, \dots, 6\}$ .
2. In such cases,

$$f_{\gamma_i} = \begin{cases} 1 + T^{\omega(\gamma_i)} z^{\partial \gamma_i} & \text{if } i \text{ odd,} \\ (1 + T^{\omega(\gamma_i)} z^{\partial \gamma_i})^2 & \text{if } i \text{ even.} \end{cases}$$

3. If we choose the branch cut between  $l_{\gamma_1}$  and  $l_{\gamma_6}$ , then the counter-clockwise monodromy  $M$  across the branch cut is given by

$$\begin{aligned} \gamma'_1 &\mapsto -(\gamma'_1 + \gamma'_2 + \gamma'_3) \\ \gamma'_2 &\mapsto \gamma'_1 + \gamma'_2 \\ \gamma'_3 &\mapsto \gamma'_1 + \gamma'_3. \end{aligned} \tag{50}$$

Notice that from the condition  $Z_{\gamma'_2} = Z_{\gamma'_3}$ , we have  $l_{\gamma'_2} = l_{\gamma'_3}$  and  $l_{\gamma'_1 + \gamma'_2} = l_{\gamma'_1 + \gamma'_3}$ . Then we compute the central charges  $Z_{\gamma_i}$ , which is parallel to Lemma 5.6. Taking the branch cut between  $l_{\gamma_1}$  and  $l_{\gamma_6}$ , we would obtain the diagram as in Figure 10.

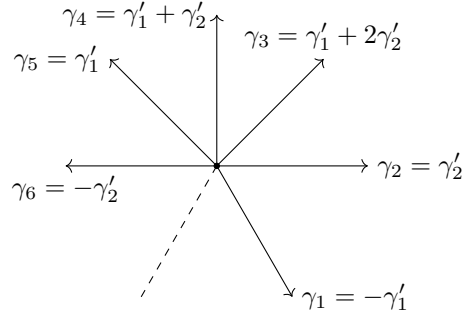


Figure 10: BPS rays near the singular fibre in  $X_{III}$ .

**Lemma 6.2.** *With suitable choice of coordinate  $u$  on  $B_0 \cong \mathbb{C}^*$ , we have*

$$Z_{\gamma_k}(u) = \begin{cases} e^{\pi i(k-1)\frac{3}{4}} u^{\frac{3}{4}} & \text{if } k \text{ odd,} \\ \frac{1-i}{2} e^{\pi i(k-2)\frac{3}{4}} u^{\frac{3}{4}} & \text{if } k \text{ even.} \end{cases} \tag{51}$$

In particular, the angle between  $l_{\gamma_k}$  and  $l_{\gamma_{k+1}}$  is  $\frac{\pi}{3}$ . See how the BPS rays position as demonstrated in Figure 10.

*Proof.* Straight-forward calculation shows that  $Z_{\gamma_k}(u) = O(|u|^{\frac{3}{4}})$ . Normalize the coordinate  $u$  such that  $Z_{\gamma_1}(u) = u^{\frac{3}{4}}$ . Notice that  $M\gamma_k = \gamma_{k+2}$ , the case for  $k$  being odd follows immediately. Similarly, when  $k$  is even,  $Z_{\gamma_k}(u) = ce^{\pi i(k-2)\frac{3}{4}} u^{\frac{3}{4}}$ , for some  $c \in \mathbb{C}$ . With  $Z_{\gamma_2} + Z_{\gamma_4} = Z_{\gamma_3}$  we get  $c = \frac{1-i}{2}$ .  $\square$

We will take  $U_i$  be the sector bounded by  $l_{\gamma_i}$  and  $l_{\gamma_{i+1}}$ . Let  $\check{X}$  to be the family Floer mirror constructed by Tu [44]. Again we denote the embedding  $\alpha_i : \mathfrak{Trop}_i^{-1}(U_i) \rightarrow \check{X}$ . From Lemma 6.2,  $x_i > 0$  on a sector symmetric with respect to  $l_{\gamma_i}$  and angle  $\frac{2\pi}{3} \times 2$ . Thus,  $\alpha_i$  can be extended to  $\mathfrak{Trop}_i^{-1}\left(\overline{\bigcup_{k=i-2}^{k=i+2} U_k}\right)$ . Following the same line of Lemma 5.14 and Lemma 5.15,  $\alpha_i$  extends to  $\mathfrak{Trop}^{-1}\left(\overline{\bigcup_{k=i-2}^{k=i+3} U_k}\right)$ . Finally,  $\alpha_i$  extends over  $l_{\gamma_{i+4}}$  from the following analogue of Lemma 5.16. The proof is similar and we will omit the proof.

**Lemma 6.3.** *The composition of the wall-crossing transformations cancel out the monodromy. Explicitly,*

$$\mathcal{K}_{\gamma_6} \mathcal{K}_{\gamma_5} \mathcal{K}_{\gamma_4} \mathcal{K}_{\gamma_3} \mathcal{K}_{\gamma_2} \mathcal{K}_{\gamma_1}(z^\gamma) = z^{M^{-1}\gamma}.$$

Similar to the argument of Section 5.3, we may change the branch cut in Figure 10 into two, as in Figure 11. The explicit gluing functions of  $B_2$ -cluster variety can be found in [6, p.54 Figure 4.1]. Then the family Floer mirror  $\check{X}$  can be partially compactified to gluing of six tori (up to GAGA) with the gluing function same as the  $\mathcal{X}$  cluster variety of type  $B_2$ . One can compute the product of the theta functions via broken lines and obtain

$$\begin{aligned} \vartheta_{v_1} \vartheta_{v_3} &= 1 + \vartheta_{v_2}, \\ \vartheta_{v_2} \vartheta_{v_4} &= (1 + \vartheta_{v_3})^2, \\ \vartheta_{v_3} \vartheta_{v_5} &= 1 + \vartheta_{v_4}, \\ \vartheta_{v_4} \vartheta_{v_6} &= (1 + \vartheta_{v_5})^2, \\ \vartheta_{v_5} \vartheta_{v_1} &= 1 + \vartheta_{v_6}, \\ \vartheta_{v_6} \vartheta_{v_2} &= (1 + \vartheta_{v_1})^2, \end{aligned} \tag{52}$$

where  $v_i$  denotes the primitive generator of  $l_{\gamma_i}$  for  $i \in \{1, \dots, 6\}$  ordered cyclically. By [7], Cheung and Magee showed that the compactification of the cluster variety of type  $B_2$  is the del Pezzo surface of degree 6.

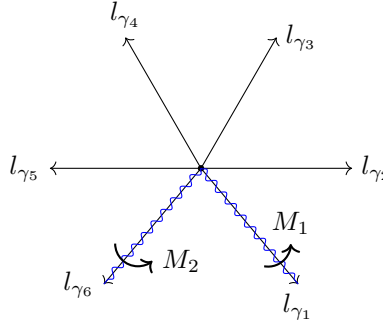


Figure 11: The choice of a different branch cut for  $X_{III}$ .

To compare with the mirror constructed by Gross-Hacking-Keel, we take the corresponding log Calabi-Yau pair  $(Y, D)$  with  $Y$  the del Pezzo surface of degree six. Since all del Pezzo surfaces of degree 6 are isomorphic, we will identify it with the blow up of  $\mathbb{P}^2$  at three points, two non-toric points on  $y$ -axis and one non-toric point on  $x$ -axis. The anti-canonical divisor  $D$  is the proper transform of the  $x, y, z$ -axis of  $\mathbb{P}^2$ . Denote  $H$  be the pull-back of the hyperplane class,  $E_1$ , (and  $E_2, E_3$ ) be the exceptional divisor of the blow up on  $x$ -axis (and  $y$ -axis).

**Lemma 6.4.** *There is an isomorphism of affine manifolds  $B_{\text{GHK}} \cong B$ .*

*Proof.* From [24, Lemma 1.6], toric blow-ups corresponds to the refinement of cone decomposition but not change the integral affine structure. We will find a successive toric blow-ups of  $(\tilde{Y}, \tilde{D}) \rightarrow (Y, D)$  such that not only the corresponding integral affine structure with singularity coincides with  $B$  but also its cone

decomposition coincide with the chamber structure bounded by the BPS rays. Such  $\tilde{Y}$  is the ordered blow up the intersection point of the  $x, z$ -axis, the proper transform of the  $z$ -axis and the exceptional divisor, the proper transform of  $y, x$ -axis. Then we take  $\tilde{D}$  to be the pull-back of the  $x, y, z$ -axis. If we take the proper transform of  $y$ -axis as  $\tilde{D}_1$  and number the boundary divisors in counter-clockwise order, then we have  $\tilde{D}_i^2 = -1$  if  $i$  odd and  $\tilde{D}_i^2 = -2$  if  $i$  even.

Use (6.2), we have

$$\begin{aligned} l_{\gamma_1} &= \{\tilde{x} > 0, \tilde{y} = 0\} \\ l_{\gamma_2} &= \{\tilde{y} > 0, \tilde{x} = 0\}. \end{aligned}$$

and we will identify  $l_{\gamma_1} = \mathbb{R}_{>0}(1, 0)$  and  $l_{\gamma_2} = \mathbb{R}_{>0}(0, 1)$  and the rest of the proof is similar to that in Lemma 5.9.  $\square$

Same argument of Lemma 5.22, we have a homeomorphism between  $X_{III} \cong Y \setminus D \cong \tilde{Y} \setminus \tilde{D}$  and  $\tilde{Y}$  provides a compactification of  $X_{III}$ . For the later discussion, we will replace  $(Y, D)$  by  $(\tilde{Y}, \tilde{D})$  for the rest of the section (see Remark 2.1). Similarly, we have the identification of the short exact sequence (47).

Next we need to compute the canonical scattering diagram for  $(Y, D)$ . Let  $D_i$  be the components of  $D$  with  $D_i$  are exceptional curves when  $i$  even.

**Lemma 6.5.** *Under the identification of integral affine structures with singularities  $B \cong B_{\text{GHK}}$ , the canonical scattering diagram of Gross-Hacking-Keel coincides with the scattering diagram in Theorem 6.1 via identification  $z^{[C_i] - \phi_{\rho_i}(v_i)} = z^{\gamma_i}$  (or  $z^{[C_i^j] - \phi_{\rho_i}(v_i)} = z^{\gamma_i}$ ) for  $i$  is odd (or even).*

*Proof.* We will first compute all the  $\mathbb{A}^1$ -curves of  $(Y, D)$ , which is standard and we just include it for self-completeness. Any irreducible curves, in particular the irreducible  $\mathbb{A}^1$  curves in  $(Y, D)$  are either exceptional curves of blow-up from  $\mathbb{P}^2$  or proper transform of a curve  $C \subseteq \mathbb{P}^2$ . All the three exceptional curves are  $\mathbb{A}^1$ -curves intersecting  $D_i$  for  $i$  odd. If  $C$  is of degree one and its proper transform is an  $\mathbb{A}^1$ -curve, then it either

1. passes through two of the blow up points and its proper transform intersect  $\tilde{D}_i$  for  $i$  odd. There are three such lines.
2. passes through one blow up point and one intersection of toric 1-stratum. There are three such lines and intersect  $\tilde{D}_i$  for  $i$  even.

There are no higher degree curves with proper transform are  $\mathbb{A}^1$ -curves and we draw the canonical scattering diagram and the corresponding  $\mathbb{A}^1$ -curves in Figure 12.

Since  $D \in |-K_Y|$  is ample, there is no holomorphic curves contained in  $Y \setminus D$ . In particular, all the simple  $\mathbb{A}^1$ -curves are irreducible and all the possible  $\mathbb{A}^1$ -curves are the multiple covers of the above ones. The contribution of multiple covers of degree  $d$  is  $(-1)^{d-1}/d^2$  by [23, Proposition 6.1]. Then the lemma follows from the definition of the canonical scattering diagram [24, Definition 3.3]. Then the function attached to the ray  $\rho_i$  is

$$f_i = \begin{cases} (1 + z^{[C_i] - \phi_{\rho_i}(v_i)}), & \text{if } i \text{ is odd,} \\ \prod_{j=1}^2 (1 + z^{[C_i^j] - \phi_{\rho_i}(v_i)}), & \text{if } i \text{ is even,} \end{cases} \quad (53)$$

where  $C_i, C_i^j$  are the  $\mathbb{A}^1$ -curve classes corresponding to  $l_{\gamma_i}$  in Figure 12. The assumption  $Z_{\gamma_2} = Z_{\gamma_3}$  implies that  $z^{[E_2]} = z^{[E_3]}$ . Notice that the monodromy of the only singular fibre shifts  $\gamma_i$  to  $\gamma_{i+2}$ . This implies that one would also need to identify

$$\begin{aligned} z^{[E_1]} &= z^{[H-E_i]} = z^{[2H-E_1-E_2-E_3]} \\ z^{[E_i]} &= z^{[H-E_i]} = z^{[H-E_1-E_i]}, i = 2, 3. \end{aligned}$$

Equivalently, this corresponds to

$$z^{[D_i]} = z^{[C_i]} = z^{[C_i^j]} = 1.$$

$\square$



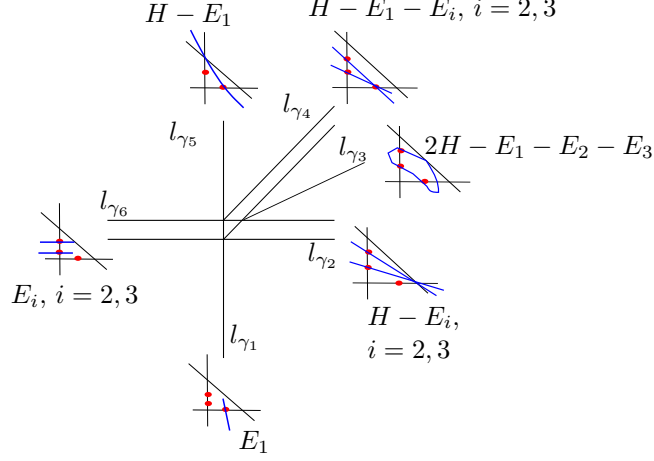


Figure 12: The canonical scattering diagram and the  $\mathbb{A}^1$ -curves in del Pezzo surfaces of degree 6 (illustrated by a projection to  $\mathbb{P}^2$ ).

The GHK mirror can be computed via the spectrum of the algebra generated by theta functions. The products of the theta functions

$$\begin{aligned} \vartheta_{i-1}\vartheta_{i+1} &= z^{[D_i]} \prod_{j=1}^2 \left( \vartheta_i + z^{[C_i^j]} \right) \quad \text{for } i \text{ even,} \\ \vartheta_{i-1}\vartheta_{i+1} &= z^{[D_i]} \left( \vartheta_i + z^{[C_i]} \right) \quad \text{for } i \text{ odd.} \end{aligned}$$

Again compare it with the analogue relations (52) from  $\mathcal{X}$ -cluster algebra of type  $B_2$ , we conclude that the family Floer mirror  $\tilde{X}$  corresponds to the particular fibre of the GHK mirror characterized by

$$z^{[D_i]} = z^{[C_i]} = z^{[C_i^j]} = 1.$$

To sum up, we conclude the section with the following theorem.

**Theorem 6.6.** *The family Floer mirror of  $X_{III}$  has a partial compactification as the analytification of the  $B_2$ -cluster variety or the Gross-Hacking-Keel mirror of suitable pair  $(Y, D)$ . In particular, the family Floer mirror of  $X_{III}$  can be compactified as the analytification of a del Pezzo surface of degree 6.*

## 7 Family Floer Mirror of $X_{IV}$

In this section, we will consider the case when  $Y'$  be a rational elliptic surface with singular configuration  $IV^*IV$  and  $D'$  is the type  $IV^*$  fibre. We claim that the family Floer mirror of  $X$  is then the del Pezzo surface of degree 4. The argument is also similar to that in Section 5. Such rational elliptic surface  $Y'$  has Weiestrass model

$$y^2 = x^3 + t^2 s^4. \tag{54}$$

**Theorem 7.1.** [39, Theorem 4.14] *There exist  $\gamma'_1, \gamma'_2, \gamma'_3, \gamma'_4 \in H_2(X, L_u) \cong \mathbb{Z}^4$  such that  $\langle \gamma'_1, \gamma'_i \rangle = 1$ ,  $\langle \gamma'_i, \gamma'_j \rangle = 0$  and  $Z_{\gamma'_i} = Z_{\gamma'_j}$ , for  $i, j \in \{2, 3, 4\}$ . Moreover, if we set*

$$\begin{aligned} \gamma_1 &= -\gamma'_1, \quad \gamma_2 = \gamma'_2, \quad \gamma_3 = \gamma'_1 + \gamma'_2 + \gamma'_3 + \gamma'_4, \quad \gamma_4 = \gamma'_1 + \gamma'_2 + \gamma'_3, \\ \gamma_5 &= 2\gamma'_1 + \gamma'_2 + \gamma'_3 + \gamma'_4, \quad \gamma_6 = \gamma'_1 + \gamma'_2, \quad \gamma_7 = \gamma'_1, \quad \gamma_8 = -\gamma'_4. \end{aligned}$$

Then

1.  $f_\gamma(u) \neq 1$  if and only if  $u \in l_{\gamma_i}$  and  $\gamma = \gamma_i$  for some  $i \in \{1, \dots, 8\}$ .
2. In such cases,

$$f_{\gamma_i} = \begin{cases} 1 + T^{\omega(\gamma_i)} z^{\partial \gamma_i} & \text{if } i \text{ odd,} \\ (1 + T^{\omega(\gamma_i)} z^{\partial \gamma_i})^3 & \text{if } i \text{ even.} \end{cases}$$

3. If we choose the branch cut between  $l_{\gamma_1}$  and  $l_{\gamma_8}$ , then the counter-clockwise monodromy  $M$  across the branch cut is given by

$$\begin{aligned} \gamma'_1 &\mapsto -(\gamma'_1 + \gamma'_2 + \gamma'_3 + \gamma'_4) \\ \gamma'_2 &\mapsto \gamma'_1 + \gamma'_2 \\ \gamma'_3 &\mapsto \gamma'_1 + \gamma'_3 \\ \gamma'_4 &\mapsto \gamma'_1 + \gamma'_4. \end{aligned} \tag{55}$$

$$\tag{56}$$

**Lemma 7.2.** With suitable choice of coordinate  $u$  on  $B_0 \cong \mathbb{C}^*$ , we have

$$Z_{\gamma_k}(u) = \begin{cases} e^{\frac{5\pi}{6}i(k-1)} u^{\frac{2}{3}} & \text{if } k \text{ odd,} \\ \frac{1}{\sqrt{3}} e^{\frac{5\pi}{6}i(k-1)} e^{-\frac{\pi i}{6}} u^{\frac{2}{3}} & \text{if } k \text{ even.} \end{cases} \tag{57}$$

In particular, the angle between  $l_{\gamma_i}$  and  $l_{\gamma_{i+1}}$  is  $\frac{\pi}{4}$ . See how the BPS rays position as demonstrated in Figure 13.

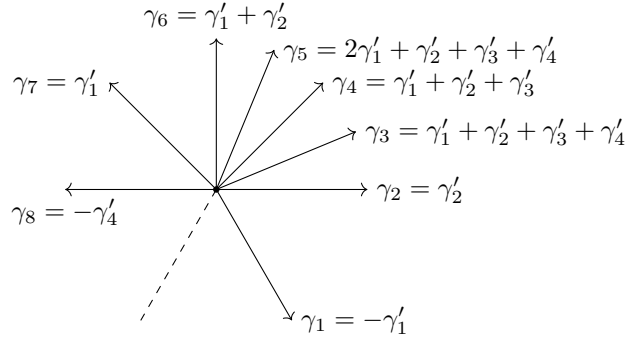


Figure 13: BPS rays near the singular fibre in  $X_{IV}$ . Note in Theorem 7.1, we have  $Z_{\gamma'_i} = Z_{\gamma'_j}$ , for  $i, j \in \{2, 3, 4\}$ .

*Proof.* One can check that  $Z_\gamma(u) = O(|u|^{\frac{2}{3}})$  and let  $Z_{\gamma_k}(u) = c_k u^{\frac{2}{3}}$ . Using the relations between  $\gamma_i$  and straight-forward calculation show that

$$c_1 = 1, c_2 = \frac{1}{\sqrt{3}} e^{-\frac{\pi i}{6}}, c_3 = e^{-\frac{\pi i}{3}}, c_4 = -\frac{i}{\sqrt{3}}$$

after suitable normalization of the coordinate  $u$ . Then use the relation  $M_{\gamma_i} = \gamma_{i+4}$  to determines the rest of  $c_k$ .  $\square$

With the data above, the similar argument in Section 5.1 shows that the family Floer mirror of  $X_{IV}$  is gluing of eight copies of  $\mathfrak{Trop}(\mathbb{R}^2 \setminus \{0\}) \subseteq (\mathbb{G}_m^{an})^2$ , with the gluing functions in Theorem 7.1. Similar to the argument of Section 5.3, we may change the branch cut in Figure 13 into two, as in Figure 14.

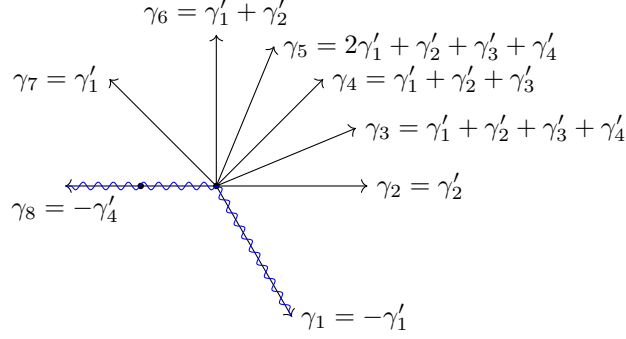


Figure 14: A choice of a different branch cut for  $X_{IV}$

The scattering diagram of cluster type  $G_2$  can be found in [26, Figure 1.2]. One can show that the corresponding gluing functions of the  $\mathcal{X}$  case are the same as those in Theorem 7.1 under suitable identification. Then the family Floer mirror of  $X_{IV}$  can be partially compactified to gluing of eight tori (up to GAGA) with the gluing functions same as the  $\mathcal{X}$ -cluster variety of type  $G_2$ .

Next we will construct a log Calabi-Yau pair  $(Y, D)$  such that the corresponding Gross-Hack-Keel mirror corresponds to the family Floer mirror of  $X_{IV}$ . We will take

1.  $Y$  to be the blow up of  $\mathbb{P}^2$  at 4 points, three of them are the non-toric points on  $y$ -axis and one non-toric point on  $x$ -axis.
2.  $D$  is the proper transform of  $x, y, z$ -coordinate axis.

Let  $\tilde{Y}$  be the successive toric blow up of  $(Y, D)$  at the intersection of  $x, z$ -axis, the proper transform of  $z$ -axis and the exceptional divisor, the two nodes on the last exceptional divisor and then the proper transform of  $y, z$ -axis in order. Then take  $\tilde{D}$  to be the proper transform of  $D$ . Denote  $H$  to be the pull-back of the hyperplane class on  $\mathbb{P}^2$ ,  $E_1$  (and  $E_2, E_3, E_4$ ) to be the exceptional divisor of the blow up on the non-toric point on the  $x$ -axis (and  $y$ -axis).

Similar to the argument Section 5.2 we have the following lemma.

**Lemma 7.3.** *The complex affine structure on  $B_0$  together with  $l_{\gamma_i}$  is isomorphic to the integral affine manifold  $B_{\text{GHK}}$  of  $(\tilde{Y}, \tilde{D})$ . Moreover, the BPS rays  $l_{\gamma_i}$  give the correoding cone decomposition on  $B_{\text{GHK}}$  from  $(\tilde{Y}, \tilde{D})$ , the wall function with restriction  $z^{[D_i]} = z^{[E_i]} = 1$  and the identification  $d$  coincide with the functions in Theorem 7.1*

We then can compute the canonical scattering diagram for  $(Y, D)$ . Actually all the simple  $\mathbb{A}^1$ -curves contributing to the scattering diagram are toric transverse in  $(\tilde{Y}, \tilde{D})$ , which are depicted in Figure 15 below.

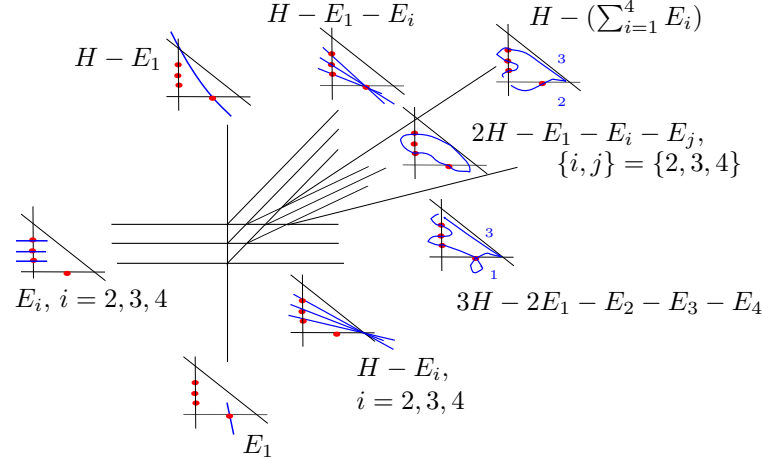


Figure 15: The canonical scattering diagram and the  $\mathbb{A}^1$ -curves corresponding to  $X_{IV}$  (illustrated by a projection to  $\mathbb{P}^2$ ).

We conclude the section with the following theorem.

**Theorem 7.4.** *The family Floer mirror of  $X_{IV}$  has a partial compactification as the analytification of the  $G_2$ -cluster variety or the Gross-Hacking-Keel mirror of a suitable pair  $(Y, D)$ .*

## 8 Further Remarks

Here we consider the family Floer mirror of  $X$  without the geometry of its compactification. Following the idea of the Gross-Hacking-Keel as summarized in Section 2.1, one would need to use the theta functions, the tropicalization of the counting of Maslov index two discs, to construct a (partial) compactification of the original mirror. Assuming that  $X = X_*$  in the previous sections admit a compactification to a rational surface with an anti-canonical cycle at infinity. Moreover, assume that there is certain compatibility between the compactification and the asymptotic of the metric behaviour. Then one can follow the similar argument in the work of the second author [37] and prove that the counting of the Maslov index two discs with Lagrangian fibre boundary conditions can be computed by the weighted count of broken lines. However, the authors are unaware of such asymptotic estimates of the metrics in the literature.

One can further construct the pair  $(Y, D)$  such that the corresponding monodromy is conjugate to the monodromy of the type  $IV^*, III^*, II^*, I_0^*$ . For instance, the case of  $I_0^*$  can be realized by a cubic surface with anti-canonical cycle consisting of three  $(-1)$ -curves [27]. The authors would expect that the family Floer mirror of  $X = Y \setminus D$  coincides with a particular fibre in the mirror family constructed by Gross-Hacking-Keel. Moreover, the families of Maslov index zero discs emanating from the singular fibres in  $X$  are one-to-one corresponding to the  $\mathbb{A}^1$ -curves of the pair  $(Y, D)$ . This may help to understand the Floer theory of more singular Lagrangians. In this case, the wall functions are algebraic functions and the GAGA can still apply. Although the walls are dense, it is likely the mirror can be covered by finitely many tori up to some codimension two locus. In general, the wall functions may not be algebraic a priori and GAGA may not apply directly. The authors will leave it for the future work.

## References

- [1] M. Abouzaid, *Family Floer cohomology and mirror symmetry*, Proceedings of the International Congress of Mathematicians—Seoul 2014. Vol. II, 2014, pp. 813–836.
- [2] ———, *The family floer functor is faithful*, Journal of the European Mathematical Society **19** (2017), no. 7, 2139–2217.
- [3] ———, *Homological mirror symmetry without corrections*, arXiv preprint arXiv:1703.07898 (2017).
- [4] D. Auroux, *Special lagrangian fibrations, wall-crossing, and mirror symmetry* (2009), 1–47.
- [5] P. Boalch, *Wild character varieties, meromorphic Hitchin systems and Dynkin diagrams*, Geometry and physics. Vol. II, 2018, pp. 433–454.

- [6] M.-W. Cheung, *Tropical techniques in cluster theory and enumerative geometry*, Ph.D. Thesis, 2016.
- [7] M.-W. Cheung and T. Magee, *Towards Batyrev duality for finite-type cluster varieties*. in preparation.
- [8] M.-W. Cheung, T. Magee, and A. N. Chávez, *Compactifications of cluster varieties and convexity*, International Mathematics Research Notices (2020).
- [9] M.-W. M. Cheung and R. Vianna, *Algebraic and symplectic viewpoint on compactifications of two-dimensional cluster varieties of finite type*, arXiv preprint arXiv:2008.03265 (2020).
- [10] T. Collins, A. Jacob, and Y.-S. Lin, *Special Lagrangian submanifolds of log Calabi-Yau manifolds*, arXiv: 1904.08363, to appear in Duke. Math. J.
- [11] ———, *The SYZ mirror symmetry conjecture for del pezzo surfaces and rational elliptic surfaces*, preprint 2020, arXiv: 2012.05416.
- [12] B. Conrad, *Several approaches to non-Archimedean geometry, p-adic geometry*, 2008, pp. 9–63.
- [13] M. Einsiedler, M. Kapranov, and D. Lind, *Non-Archimedean amoebas and tropical varieties*, J. Reine Angew. Math. **601** (2006), 139–157.
- [14] B. Fang, C.-C. M. Liu, D. Treumann, and E. Zaslow, *T-duality and homological mirror symmetry for toric varieties*, Adv. Math. **229** (2012), no. 3, 1875–1911.
- [15] S. Fomin and A. Zelevinsky, *Cluster algebras I: Foundations*, J. Amer. Math. Soc. **15** (2002), 497–529.
- [16] L. Fredrickson, R. Mazzeo, J. Swoboda, and H. Weiss, *Asymptotic geometry of the moduli space of parabolic  $SL(2, \mathbb{C})$ -Higgs bundles*, preprint 2020, arXiv:2001.03682.
- [17] K. Fukaya, *Multivalued morse theory, asymptotic analysis and mirror symmetry, graphs and patterns in mathematics and theoretical physics, 205–278*, Proc. sympos. pure math.
- [18] ———, *Floer homology for families—a progress report*, Integrable systems, topology, and physics (Tokyo, 2000), 2002, pp. 33–68.
- [19] ———, *Cyclic symmetry and adic convergence in Lagrangian Floer theory*, Kyoto J. Math. **50** (2010), no. 3, 521–590.
- [20] K. Fukaya, Y.-G. Oh, H. Ohta, and K. Ono, *Lagrangian intersection Floer theory: anomaly and obstruction. Part II*, AMS/IP Studies in Advanced Mathematics, vol. 46, American Mathematical Society, Providence, RI, 2009.
- [21] D. Gaiotto, G. W Moore, and A. Neitzke, *Wall-crossing, Hitchin systems, and the WKB approximation*, Advances in Mathematics **234** (2013), 239–403.
- [22] Y. Groman, *Y groman, floer theory and reduced cohomology on open manifolds*, preprint 2015, arXiv: 1510.04265.
- [23] M. Gross, R. Pandharipande, and B. Siebert, *The tropical vertex*, Duke Math. J. **153** (2010), no. 2, 297–362.
- [24] M. Gross, P. Hacking, and S. Keel, *Mirror symmetry for log Calabi-Yau surfaces I*, Publ. Math. Inst. Hautes Études Sci. **122** (2015), 65–168.
- [25] ———, *Birational geometry of cluster algebras*, Algebr. Geom. **2** (2015), no. 2, 137–175.
- [26] M. Gross, P. Hacking, S. Keel, and M. Kontsevich, *Canonical bases for cluster algebras*, J. Amer. Math. Soc. **31** (2018), no. 2, 497–608.
- [27] M. Gross, P. Hacking, S. Keel, and B. Siebert, *The mirror of the cubic surface*, 2019.
- [28] M. Gross and B. Siebert, *From real affine geometry to complex geometry*, Annals of mathematics (2011), 1301–1428.
- [29] R. Harvey and H. B. Lawson Jr., *Calibrated geometries*, Acta Math. **148** (1982), 47–157.
- [30] H.-J. Hein, *Gravitational instantons from rational elliptic surfaces*, J. Amer. Math. Soc. **25** (2012), no. 2, 355–393.
- [31] N. J. Hitchin, *The moduli space of special lagrangian submanifolds*, Ann. Scuola Norm. Sup. Pisa Cl. Sci. (4) **25** (1997), no. 3-4, 503–515 (1998). Dedicated to Ennio De Giorgi.
- [32] M. Kontsevich and Y. Soibelman, *Affine structures and non-archimedean analytic spaces*, The unity of mathematics, 2006, pp. 321–385.
- [33] S.-C. Lau, T.-J. Lee, and Y.-S. Lin, *Complex affine structures of SYZ fibrations in del Pezzo surfaces*, In preparation.
- [34] ———, *On the complex affine structures of syz fibration of del Pezzo surfaces*, preprint, arXiv:2005.04825.
- [35] N. C. Leung, S.-T. Yau, and E. Zaslow, *From special Lagrangian to Hermitian-Yang-Mills via Fourier-Mukai transform*, Winter School on Mirror Symmetry, Vector Bundles and Lagrangian Submanifolds (Cambridge, MA, 1999), 2001, pp. 209–225.
- [36] Y. Li, *SYZ conjecture for Calabi-Yau hypersurfaces in the Fermat family*, preprint 2019, arXiv:1912.02360.
- [37] Y.-S. Lin, *Enumerative geometry of del pezzo surfaces*, preprint 2020, arXiv: 2005.08681.
- [38] ———, *Open Gromov-Witten invariants on elliptic K3 surfaces and wall-crossing*, Comm. Math. Phys. **349** (2017), no. 1, 109–164.
- [39] ———, *On the tropical discs counting on elliptic k3 surfaces with general singular fibres*, Trans. Amer. Math. Soc. **373** (2020), no. 2, 1385–1405.
- [40] ———, *Correspondence theorem between holomorphic discs and tropical discs on K3 surfaces*, J. Diff. Geom. **117** (2021), no. 1, 41–92.

- [41] R. Miranda and U. Persson, *On extremal rational elliptic surfaces*, Math. Z. **193** (1986), no. 4, 537–558.
- [42] L. Shen, E. Zaslow, and P. Zhou, private communication.
- [43] J. Tate, *Algorithm for determining the type of a singular fiber in an elliptic pencil*, Modular functions of one variable iv, 1975, pp. 33–52.
- [44] J. Tu, *On the reconstruction problem in mirror symmetry*, Adv. Math. **256** (2014), 449–478.
- [45] H. Yuan, *Family Floer program and non-archimedean SYZ mirror construction*, preprint 2020, arXiv:2003.06106.
- [46] ———, *Family Floer theory of toric manifolds and wall-crossing phenomenon*, preprint 2021, arXiv: 2101.01379.

MAN-WAI CHEUNG

DEPARTMENT OF MATHEMATICS, ONE OXFORD STREET CAMBRIDGE, HARVARD UNIVERSITY, MA 02138, USA

*e-mail*: mwcheung@math.harvard.edu

YU-SHEN LIN

DEPARTMENT OF MATHEMATICS AND STATISTICS, 111 CUMMINGTON MALL, BOSTON, BOSTON UNIVERSITY, MA 02215, USA

*e-mail*: yslin@bu.edu